MEASUREMENT OF NONLINEAR DYNAMIC PROPERTIES OF BONNEVILLE SILTY-CLAYS

NIW Program

Dr. James A. Bay

Dr. Inthourn Sasanakul

Research supported by the U.S. Geological Survey (USGS), Department of the Interior, under USGS award number 04HQGR0055. The views and conclusions contained in this document are those of the authors and should not be interpreted as necessarily representing the official policies, either expressed or implied, of the U.S. Government.

November 11, 2005

Award 04HQGR0055

MEASUREMENT OF NONLINEAR DYNAMIC PROPERTIES OF BONNEVILLE SILTY-CLAYS

Dr. James A. Bay and
Dr. Inthuorn Sasanakul

Utah State University
Department of Civil and Environmental Engineering
Logan, Utah 84322-4110
(435) 797-2947
(435) 797-1185 FAX
jim.bay@usu.edu

Technical Abstract

Resonant column and torsional shear (RC/TS) testing was performed on samples of Bonneville silty-clay from four sites around the Wasatch Front. The purpose of these tests was to measure the nonlinear modulus and damping of these soils. The report contains the details of the testing and analysis procedure including the approach used to correct for back-EMF in the RC/TS apparatus. The soils tested included soils classified as ML, CL, and CH. PI's of the soils tested ranged from 2 to 34. This range of properties is a good representation of the variability of Lake Bonneville Lacustrine soils. Empirical relationships based upon the PI of a soil and confining pressure are often used to predict nonlinear properties of soils for seismic analysis. All of the Bonneville soils exhibited more linear behavior (lower damping and less modulus reduction at a given strain) than would be predicted based upon the commonly used empirical relationships of Vucetic and Dobry (1991), Sun et al. (1988), and Darendeli (2001). Procedures to correct for this increased linearity are proposed. Using the Vucetic and Dolbry relationships with a PI value 10 higher than actual PI provides a good prediction of the behavior of Bonneville soils. A linear increase (presented in the report) in PI Darendeli's relationship also provides a good prediction of the behavior of Bonneville soils. The measurements show the same effect of confinement as predicted by Darendeli's relationship. Other relationships, such as Vucetic and Dolby and Sun, do not include the effect of confinement. One possible explanation for the more linear behavior of the Bonneville soils is their relatively young age. Many of the soils used to develop the empirical relationships are tertiary soils. Zhang et al. (2004) also show that the empirical relationships provide better predictions for tertiary soils than quaternary soils in South Carolina.

Non-Technical Abstract

Resonant column and torsional shear (RC/TS) testing was performed on samples of Bonneville silty-clay from four sites around the Wasatch Front. The purpose of these tests was to measure the dynamic properties of the soils that are used in a site-specific seismic analysis. Bonneville soils were deposited in ancient Lake Bonneville, and the properties of these soils vary significantly around the Wasatch Front. The soils tested in this study span this variability. Empirical relationships developed by several researchers are often used to predict the dynamic properties of soils for seismic analysis. This study found that Bonneville soils consistently behave quite differently than would be predicted by these empirical relationships. Bonneville soils behaved more linearly than the empirical relationships predict. This means that there will be less loss of seismic energy as earthquake waves propagate through Bonneville soils than would be predicted. Methods to correct for the differences between the measured and predicted behavior are proposed.

DYNAMIC PROPERTIES OF BONNEVILLE CLAY

1 INTRODUCTION

Resonant column (RC) and torsional shear (TS) testing was performed on Bonneville clay to develop modulus reduction curves and damping curves. Previous to this study, no measurements have been made of modulus reduction and damping in Bonneville clay. In this testing, the electromagnetic model was used to correct for equipment generated damping and the stress integration approach was used to calculate stresses and strains. This report is separated into four sections. Each section is described below.

The first section presents a description of soil specimens used in this study. Soil description includes sample depth and location, physical properties, and soil classification.

The second section presents the RC/TS testing procedures. These procedures include the specimen preparation and RC and TS testing sequences.

The third section briefly presents the RC/TS analysis procedures. These procedures include correction for equipment generated damping, and application of the stress integration approach to develop modulus reduction and damping curves.

And the fourth section presents a discussion of the factors affecting the modulus reduction and damping curves for Bonneville clay. These factors are plasticity index, confining pressure. The modulus reduction and damping of Bonneville clay are compared with generic modulus reduction and damping curves. These comparisons show that Bonneville clay behaves more linear than generic curves predict. At the end of this section, conclusions drawn from the test results are presented.

2 SOIL SPECIMENS

Bonneville clay is very soft lacustrine silty-clay deposited in Ancient Lake Bonneville. It underlies the shores of both the Great Salt Lake and Utah Lake as well as the large portions of Salt Lake Valley and adjacent valleys. Seven samples of Bonneville clay were tested in this study. They were obtained from four different sites distributed across the Wasatch front. Three samples were collected at a site near the Provo River in Utah County. One sample was from a site at Nibley in Cache County. One sample was from a site in Logan in Cache County. And, two samples were collected from a site near the Salt Lake City Airport in Salt Lake County. Locations of each site are presented in Table 1.

Undisturbed samples were recovered from the sites using thin-walled Shelby tubes. Radiographic (X-ray) images were made of all samples prior to opening sample tubes to assess the sample quality and to select portions of the sample for testing. Atterberg limits and hydrometer tests were performed on each sample to determine the soil classification and index properties of soil specimen. Other physical properties of the soil specimen were also determined prior to the RC/TS testing. The physical properties and unified soil classification are presented in Table 2.

Table 1 Sample Sites Location

Site No.	County	Address
1	Utah	Geneva Rd. Bridge over Provo River, Provo, UT
2	Cache	2835 S 1000 W Nibley, UT
3	Cache	USU Drainage Farm Site Logan, UT
4	Salt Lake	BYU Research Site North West of Salt Lake City International Airport, Salt Lake City, UT

All of the soil specimens in this study are fine-grained soils with, the percent passing the No. 200 sieve all greater than 85%. The index properties of each soil specimen are plotted on the plasticity chart as shown in Figure 1. Specimens from the site near the Provo River, PRV37 and PRV67, are low to medium plasticity silty clay (CL), except for one sample, PRV93, from the depth of 93 ft which was clayey silt with very fine sands (ML). A specimen from shallow depth, SLC14, from a site near the Salt Lake City airport is a low to medium plasticity clay (CL) and a specimen from a deeper depth, SLC35, was low plasticity silty sand (ML). Soil specimens from Nibley, NBL24, and Logan, LGN14, are high plasticity clay (CH).

3 RC/TS TESTING PROCEDURE

3.1 Specimen Preparation

The X-ray images of the sample tube were visually examined to select the best quality portions of the samples. Once a sample portion was chosen, each end of the selected portion was cut using a tube cutter. The side of the tube was then cut vertically using a band saw. In most case, the tube sprung open after cutting, and the soil was easily removed. When the tube did not spring open, the opposite side of the tube was cut to remove soil with minimal disturbance.

Soil specimens were carefully hand-trimmed to a diameter of approximately 1.4 inches and a height of about 3.0 inches using a trimming device and wire saw. Water content was determined using the trimmings. The trimmed specimen was weighed and dimensions were measured before placing the specimen on the base pedestal of the RC/TS equipment.

Next, two small circular pieces of filter paper were placed over the drainage holes on the base pedestal. The base pedestal was then secured to the base plate with four screws. The specimen was then set on the base platen and the top cap was gently placed on top of specimen. Two layers of latex membrane were then placed over the soil specimen and each layer of membrane was sealed separately with O-rings on the top cap and the base pedestal. A silicon oil bath was then placed around the specimen to minimize the diffusion of air through the membrane.

Table 2 Physical Properties of Soil Specimens

Sample ID	Site No.	Depth (ft)	Unified Soil Classification	Liquid Limit	Plasticity Index	% Passing No.200 Sieve	% Clay Size Particle < 0.002 mm	Water Content (%)	Unit Weight (pcf)	Void Ratio	Degree of Saturation (%)
PRV37	1	37	CL	43	20	99.46	16.81	30.61	113.86	0.981	85.77
PRV67	1	67	CL	33	11	85.84	8.42	22.40	123.13	0.661	89.83
PRV93	1	93	ML	41	10	97.60	16.10	41.64	115.09	1.052	99.85
NBL24	2	24	CH	63	34	99.32	24.03	53.83	106.53	1.483	99.78
LGN14	3	14	CH	65	34	98.82	19.92	60.90	101.80	1.744	91.54
SLC14	4	14	CL	42	17	98.98	9.06	41.07	114.57	1.043	99.91
SLC35	4	35	ML	27	2	89.94	7.00	22.26	117.15	0.735	76.48

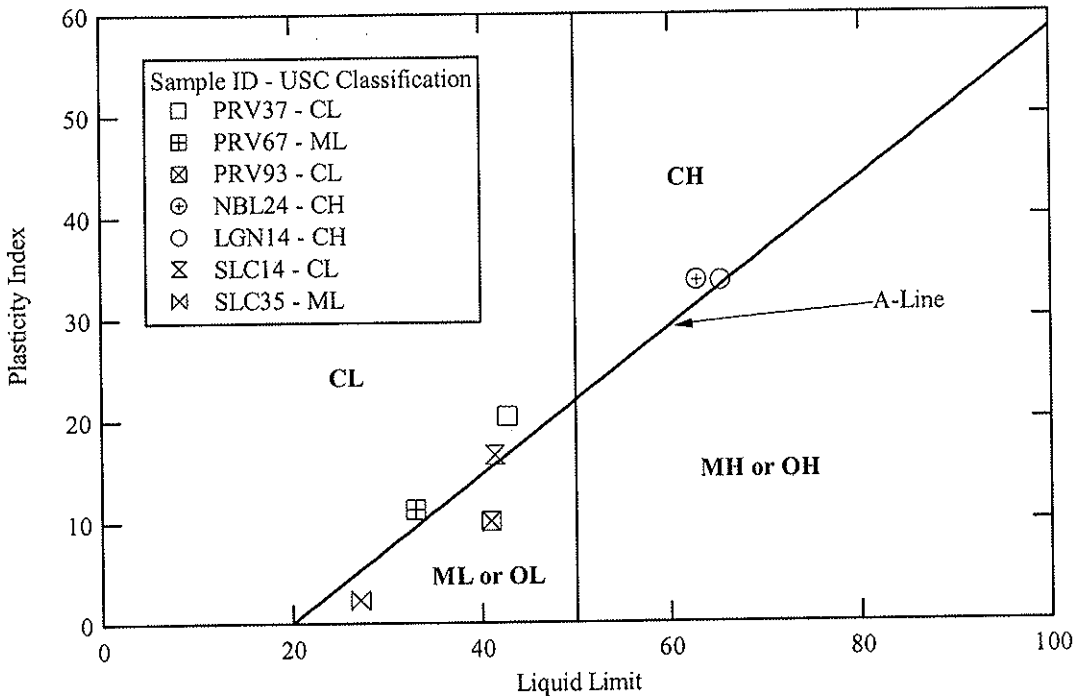

Figure 1 Unified soil classification of Bonneville clay specimens tested in this study

At this point the drive plate was attached to the top platen and the cell was positioned around the specimen and drive plate. The confining pressure was then applied and soil specimen was allowed to consolidate. When the specimen reached the end of primary consolidation, RC/TS testing was performed.

3.2 RC/TS Testing Sequence

A series of RC and TS tests were performed on soil specimens at each confining pressure. In this study, soil specimens were consolidated to the estimated mean in situ effective confining pressure (σ'_m) and two additional higher pressures at levels of $2\sigma'_m$ and $4\sigma'_m$. The RC and TS test are separated into two categories; low-amplitude tests and high-amplitude tests. The low-amplitude tests are tests at strains at which the soil specimen behaves linearly. The high amplitude tests are tests at strains where the soil acts nonlinearly. This nonlinearity can be identified from a decrease in resonant frequency in the RC test. Typically, the strain of a high-amplitude test is above 10^{-3}%. In this study, the TS testing was performed using loading frequency of 0.333 Hz for 5 cycles. The TS testing sequence is presented in Figure 2. For each confining pressure the TS tests were always performed first because the soil specimen was subjected to fewer cycles than in the RC test. However, low-amplitude RC tests were always performed before any high-amplitude TS tests to monitor any change in the small strain shear modulus (G_{max}) of the soil specimen. If the G_{max} changed significantly, the testing was paused until soil specimen returned to the original G_{max}.

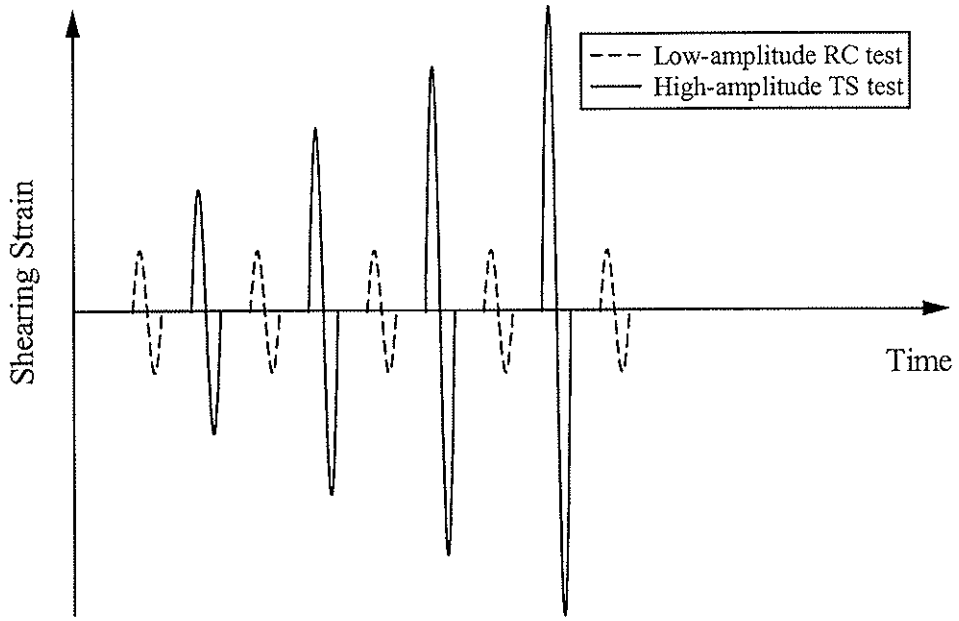

Figure 2 Testing sequence for the TS test

After finishing the last high-amplitude TS test, a low amplitude RC test was performed. The RC test sequence is presented in Figure 3. Since the soil was subjected to high strain during high-amplitude TS test, a significant decrease in the value of G_{max} was always observed after the last high-amplitude TS test. A series of low-amplitude RC test were then performed over period of time to monitor the increase in G_{max} of the soil specimen. Once the value of G_{max} was recovered to its original value (typically after at least 4 hours), the series of high strain amplitude RC tests were performed. The RC testing sequence was similar, to the TS sequence, with low amplitude RC tests performed before any high amplitude RC test. If the value of G_{max} did not return to the original value after a reasonably period of time, the change in the value of G_{max} was then recorded and the next high amplitude test was performed.

For both RC and TS tests the shear strains from less than10^{-4} to more than 10^{-1}% were applied to the soil, depending upon the soil specimen stiffness. When the high amplitude RC testing was completed the confining pressure was increased to the next level, the specimen was allowed to consolidated and the RC and TS testing sequence was repeated.

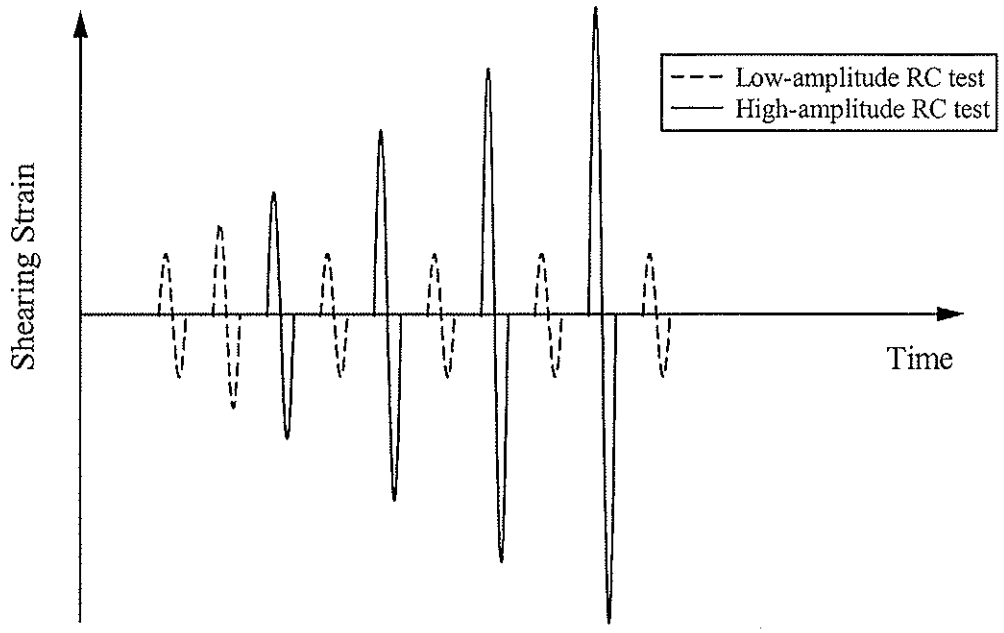

Figure 3 Testing sequence for the RC test

4 RC/TS ANALYSIS PROCEDURE

4.1 Correction for Equipment Generated Damping

The electromagnetic model was used to predict the equipment generated damping, D_{eq}, generated in the RC/TS drive system due to the back emf effect (Sasanakul 2005). According to Sasanakul (2005), the back emf effect is modeled as an additional spring and an additional dashpot creating additional stiffness and viscosity in the system. The additional stiffness, called the equipment generated spring stiffness, k_{eq}, is considered to be very small and can be neglected. The additional equipment generated viscous damping coefficient, c_{eq}, was used to calculate D_{eq}. The c_{eq} value can be predicted using:

$$c_{eq} = \frac{k_i k_B R_c}{R_c^2 + \omega^2 L_c^2} \tag{1}$$

where k_{eq} = equipment spring stiffness,
c_{eq} = equipment viscous damping coefficient,
R_c = coil resistance,
L_c = coil inductance,
k_i = torque-current factor,
k_B = back emf-rotational velocity factor, and
ω = angular velocity ($\omega = 2\pi f$).

For the RC test, the value of D_{eq} is calculated from:

$$D_{eq} = \frac{c_{eq}}{c_c}. \quad (2)$$

where c_c = critical damping coefficient ($c_c = 4\pi f_n \Sigma J$),

f_n = undamped natural frequency of specimen ($f_n = \frac{f_m}{\sqrt{1-2D^2}}$), and

ΣJ = total polar moment of inertia of the system including such as drive plate (J_o), top plate (J_t).

The model parameters, k_i, R_c and L_c have constant values of 0.318 lb-ft/rad, 45.6 ohms, and 0.0256 H, respectively. Values of k_B and J_o vary with frequency. An example of the calculations for correcting D on specimen LGN14 is presented in Table 3.

Increasing strain amplitude in RC tests results in decreasing resonant frequencies as can be seen in Table 3. The D_{eq} generated in the RC/TS drive system is inversely proportional to the resonant frequency, so as the strain amplitude increases, the D_{eq} also increases. Figure 4 shows a plot of the predicted D_{eq} versus strain for the RC test of specimen LGN14. This soil specimen is very soft with low-strain resonant frequency of about 12 Hz, and a low-strain material damping of about 2%. As shown in Table 9.3 and Figure 9.4, the calculated D_{eq} ranges from about 0.8% at low-strain amplitudes up to as high as 1.3% for high-strain amplitudes. The value of D_{eq} is almost 40% of the actual material damping at low-strains. As a result, correcting for the equipment generated damping, D_{eq}, is critical when performing low-strain RC test on low-resonant frequency soils (Sasanakul 2005).

Figure 5 shows the plot of measured D and corrected D versus strain amplitude for specimen LGN4 at confining pressure of 6.2 psi. The damping was corrected by subtracting the predicted D_{eq} from the measured D. This procedure was used to account for the equipment generated damping for all of the RC tests throughout this study.

Table 3 Example of Calculations to Correct D for Equipment Generated Damping, D_{eq}, for RC Test of Soil Specimen LGN14 from Logan, Utah

Resonant Frequency, f_m (Hz)	Shear Strain, γ (%)	Measured D (%)	J_o[1] (lb-ft-sec^2)	k_B[2] (V/rad/s)	Predicted c_{eq} (lb-ft-sec)	Calculated c_c (lb-ft-sec)	Predicted D_{eq} (%)	Corrected D (%)
11.96	1.286e-3	3.061	2.102e-3	0.3778	2.630e-3	3.178e-1	0.827	2.234
11.95	2.608e-3	3.012	2.102e-3	0.3778	2.630e-3	3.176e-1	0.828	2.184
11.88	4.962e-3	3.191	2.102e-3	0.3778	2.630e-3	3.157e-1	0.833	2.358
10.80	1.100e-2	4.503	2.102e-3	0.3777	2.630e-3	2.873e-1	0.915	3.588
10.26	1.868e-2	7.112	2.102e-3	0.3777	2.631e-3	2.737e-1	0.961	6.151
9.24	3.341e-2	10.307	2.101e-3	0.3777	2.631e-3	2.479e-1	1.061	9.246
8.24	4.494e-2	15.855	2.101e-3	0.3777	2.631e-3	2.244e-1	1.172	14.683
7.54	5.408e-2	20.595	2.101e-3	0.3777	2.632e-3	2.092e-1	1.258	19.337

Note: 1. $J_o = 0.0021013+4.673e\text{-}10 freq^{2.6798}$

2. $k_B = 0.3776+3.1227e\text{-}7 freq^{2.5307}$

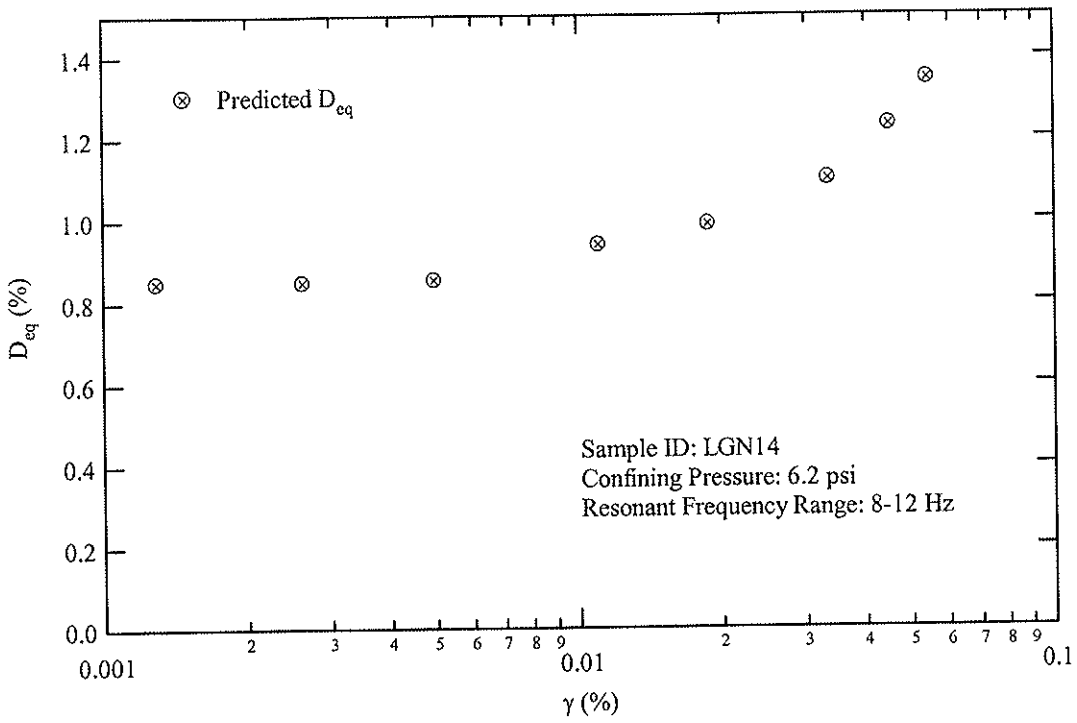

Figure 4 Predicted D_{eq} for a series of RC test on soil specimen LGN14

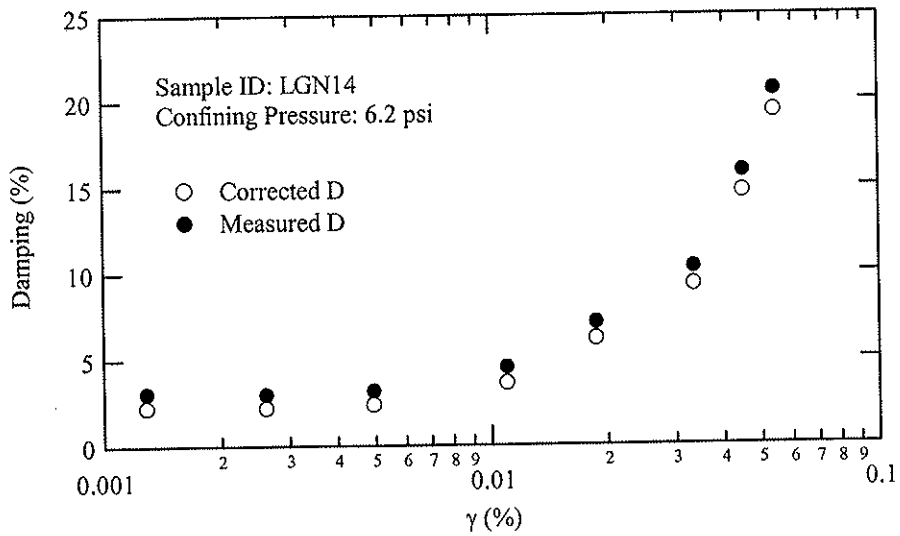

Figure 5 Measured and corrected damping for a series of RC test on soil specimen LGN14 obtained from Logan, Utah at a depth of 14 feet

4.1 Application of Stress Integration Approach

The stress integration approach developed by Sasanakul (2005) was applied to all of the RC/TS tests on Bonneville clay. This approach was developed to account for the nonuniform stresses and strains occurring over the radius of the soil specimen. The basic concept of this approach is to find a τ–γ relationship described by an assumed soil model that results in a theoretical T-θ relationships that corresponds to the measured T-θ relationship using curve fitting techniques. Details of this approach are presented in Sasanakul (2005).

The stress integration approach was used to develop modulus reduction curves and damping curves using the following procedure. (1) Perform curve fitting on the measured T- θ relation using either the closed form solution or numerical integration of each soil models. (2) Select the best soil model that provides the best fit to the experimental data. (3) Develop the modulus reduction curves based on the selected soil model and the model parameters. (4) Determine values of R_{eq} based on the hyperbolic model parameters over the range of rotations generating in testing. (5) Develop the damping curve by calculating the shear strain associated with each value of θ using the appropriate R_{eq} value.

4.2.1 Curve Fitting for T-θ Relationships and Model Selection. The measured T-θ relationships were developed from RC and TS test on seven soil samples at different confining pressures. Figures 6 and 7 show the measured and calculated values of T are plotted versus log θ so the curve fitting can be evaluated over a wide range of strains for specimen PRV93 from RC and TS tests. Curve fitting was performed on each measured T-θ relationship using three soil models; the hyperbolic, the modified hyperbolic, and the Ramberg-Osgood. The closed form solution was used to predict the T-θ relationship for the hyperbolic model while the numerical integration was used to predict the T-θ relationship for the modified hyperbolic and the Ramberg-Osgood models. This approach was applied for all soil specimen in this study.

The small strain shear modulus, G_{max} was evaluated from low strain RC/TS tests. The G_{max} value for each test was known, therefore it was constrained during the curve fitting. Summary of the model parameters and chi-square values determined from the curve fitting are presented in Table 4. The shaded fields in Table 4 are the model parameter providing the best fit.

Once the curve fitting was performed for each assumed soil model, the best fit model was selected to represent the τ–γ relationship for the soil. Chi-square is one indicator of how well the curve fitting matched the data. However, the chi-square value was always considered along with visual justification. The chi-square should be used alone only in the cases where all of assumed models match the measured T-θ relationship such that the differences cannot be distinguished visually. In this study, the best fit soil model was selected for each test individually after careful consideration.

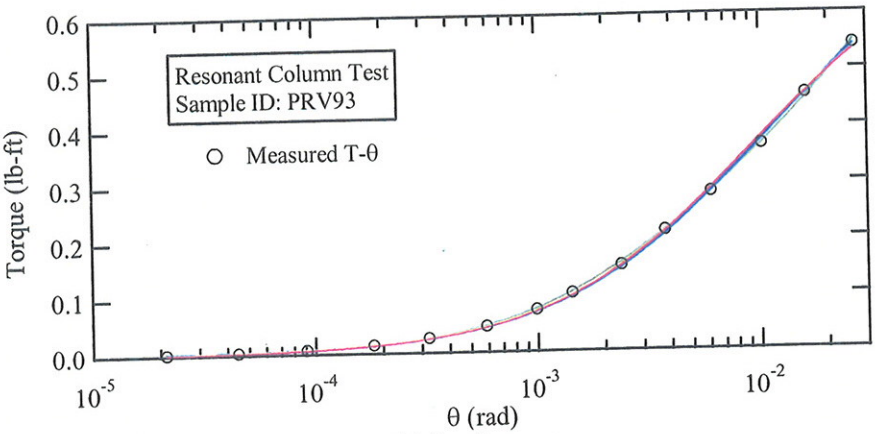

a) Confining pressure of 28 psi

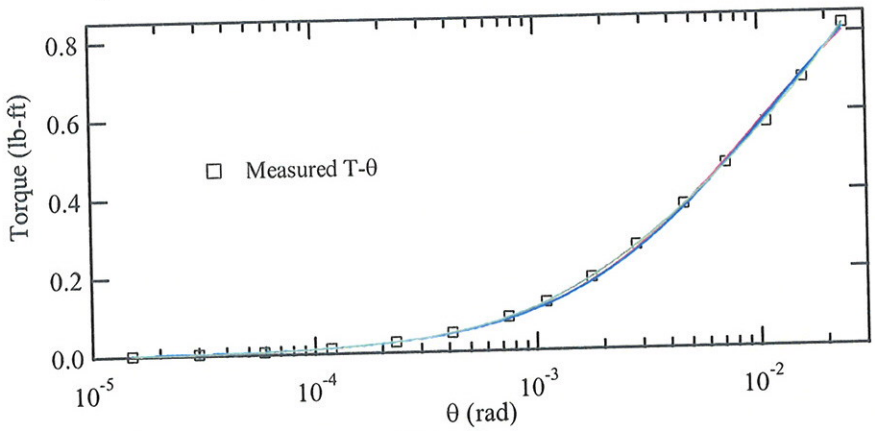

b) Confining pressure of 56 psi

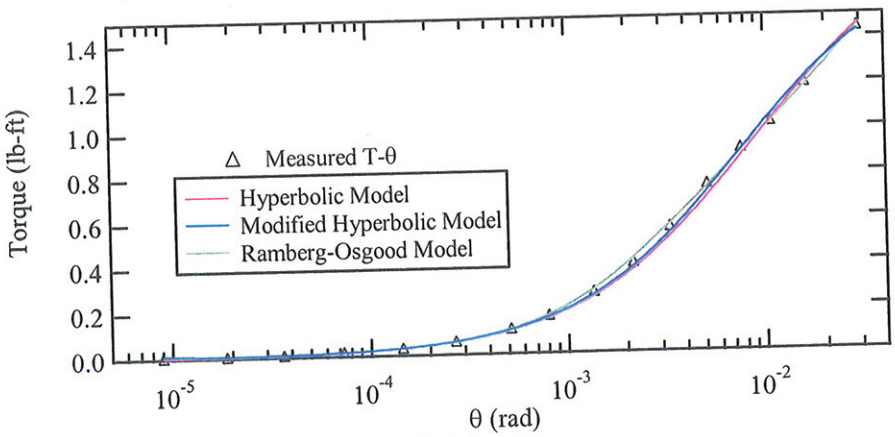

c) Confining pressure of 112 psi

Figure 6 Curve fitting for T-θ relationship for the RC tests on soil specimen PRV93 obtained near the Provo River at a depth of 93 ft

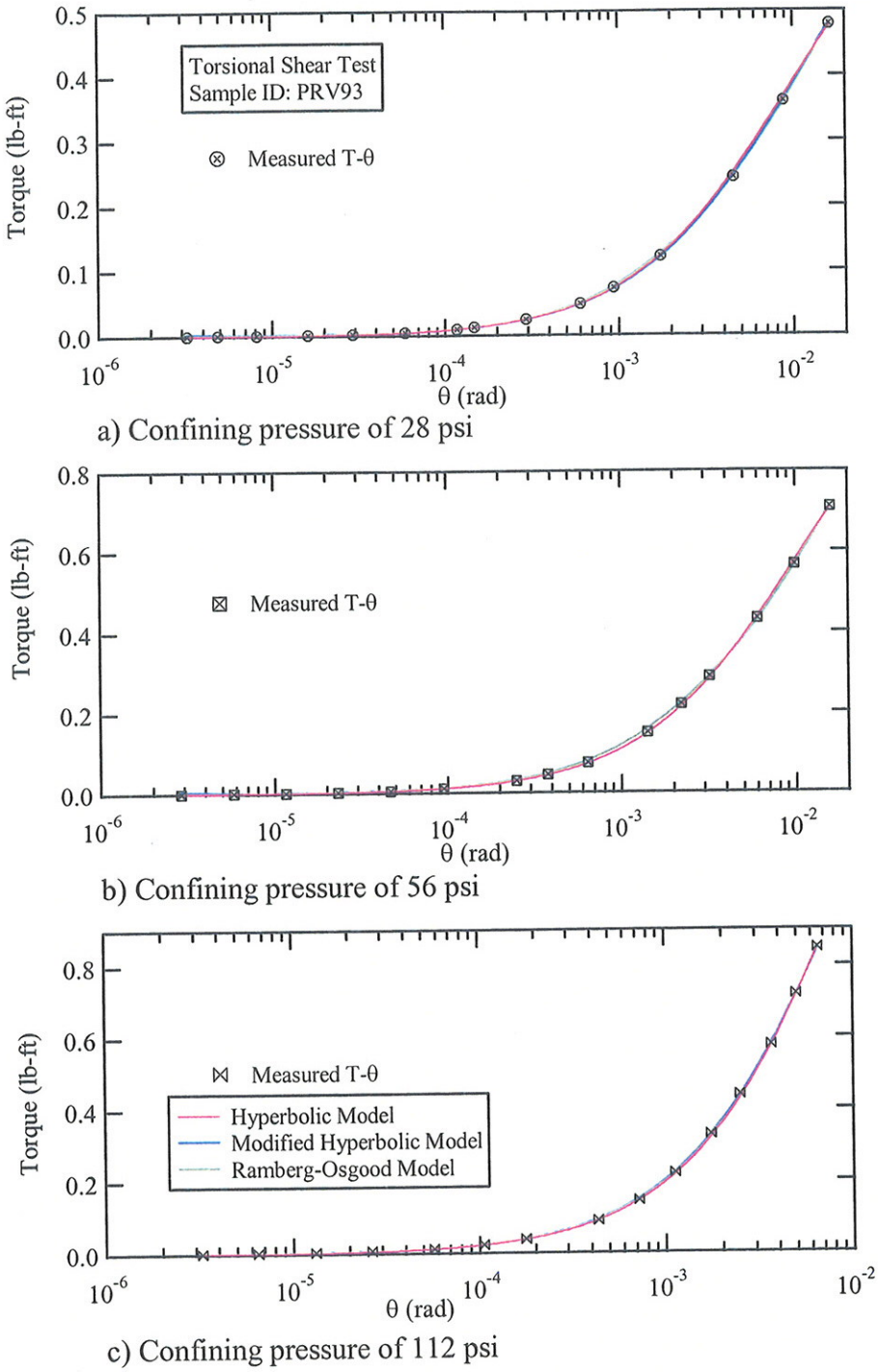

Figure 7 Curve fitting for T-θ relationship for the TS tests on soil specimen PRV93 obtained near the Provo River at a depth of 93 ft

Table 3 Curve Fitting Results from RC/TS tests on Bonneville Clay

Sample ID	Test	Confining Pressure (psi)	G_{max} (psf)	Hyperbolic Model		Modified Hyperbolic Model			Ramberg-Osgood Model			
				γ_r (%)	chi-square	γ_r (%)	a	chi-square	γ_r (%)	α	b	chi-square
PRV37	RC[1]	12.4	9.854e5	0.0682	3.755e-5	0.0686	1.1247	1.125e-5	0.0517	2.5892	3.1565	2.294e-5
		24.8	1.417e6	0.1003	1.391e-5	0.0711	1.2718	1.746e-7	0.0845	1.8386	2.8475	1.594e-7
		49.6	2.237e6	0.12024	4.311e-5	0.0975	1.2199	3.707e-8	0.0751	1.5531	2.6576	9.285e-7
PRV67	RC	20.7	1.360e6	0.0826	2.358e-5	0.0646	0.8156	1.140e-4	0.0911	5.7177	2.6408	1.115e-4
		41.4	2.369e6	0.09883	2.827e-3	0.0884	0.8848	1.703e-4	0.0943	1.5387	2.9293	4.389e-4
		82.8	4.120e6	0.1002	2.218e-4	0.0991	0.9804	1.359e-4	0.0881	3.5389	3.0348	7.820e-4
	TS	20.7	1.576e6	0.0787	1.507e-5	0.0813	0.9247	4.777e-6	0.0672	1.8889	2.3368	1.213e-5
		41.4	2.700e6	0.0890	3.909e-4	0.0837	0.9332	7.048e-5	0.0810	1.2712	2.7652	3.230e-4
		82.8	4.512e6	0.0901	1.390e-3	0.0903	0.9822	1.463e-4	0.1260	4.3452	2.4520	3.903e-4
PRV93	RC	28	1.143e6	0.1468	4.158e-4	0.1405	0.9461	1.977e-4	0.1206	3.3366	3.0810	1.245e-4
		56	1.730e6	0.1626	1.117e-3	0.1589	0.9612	9.534e-4	0.1164	1.0101	3.0471	3.234e-5
		112	3.406e6	0.1496	6.555e-3	0.1575	1.0676	3.758e-3	0.0725	0.8989	3.9020	1.383e-3
	TS	28	1.191e6	0.1447	1.274e-4	0.1397	0.9245	2.171e-6	0.0917	1.7197	2.7414	5.821e-5
		56	1.750e6	0.1621	1.251e-4	0.1618	0.9957	1.455e-4	0.1130	1.2465	2.6823	1.884e-4
		112	3.388e6	0.1750	1.910e-4	0.1665	1.0905	6.015e-5	0.0520	0.4246	2.6025	7.282e-5
NBL24	RC	7.4	4.985e5	0.1233	2.251e-5	0.1105	0.8179	1.334e-6	0.0860	1.9180	2.2430	1.188e-7
		14.8	6.012e5	0.2041	1.432e-4	0.2338	0.6307	2.804e-5	0.1652	1.1277	1.8279	2.231e-5
		29.6	8.053e5	0.1907	4.766e-4	0.1784	0.9231	2.215e-4	0.0983	1.3168	2.9929	4.862e-5
	TS	7.4	4.790e5	0.1454	4.439e-7	0.1903	0.8268	1.334e-7	0.1387	1.1602	1.9624	1.534e-7
		14.8	5.920e5	0.1607	1.627e-7	0.3564	0.7183	6.790e-8	0.1667	0.5338	1.6435	4.149e-8
		29.6	7.500e6	0.1736	1.1207e-5	0.1708	0.9196	7.085e-5	0.0089	1.1244	2.4910	2.154e-6
LGN14	RC	6.2	1.900e5	0.1499	8.807e-6	0.1190	0.7200	4.263e-6	0.1660	3.7006	2.2539	8.051e-7
		12.4	4.130e5	0.1309	9.038e-5	0.1160	0.9101	1.354e-5	0.2011	3.0293	3.2337	1.498e-5
		24.8	8.810e5	0.0845	2.055e-4	0.0924	1.1340	5.800e-5	0.0583	2.4987	4.1770	5.050e-5
	TS	6.2	2.050e5	0.1148	1.463e-6	0.1206	0.8130	1.491e-7	0.1895	3.6054	2.1361	2.504e-7
		12.4	4.530e5	0.1251	1.127e-5	0.1176	0.9104	3.888e-6	0.2278	2.8652	2.6826	1.305e-6
		24.8	9.350e5	0.0909	4.658e-5	0.0973	1.0986	8.159e-6	0.0682	2.9783	3.7016	3.390e-5

Table 3 (continued)

Sample Location	Test	Confining Pressure (psi)	G_{max} (psf)	Hyperbolic Model		Modified Hyperbolic Model			Ramberg-Osgood Model			
				γ_r (%)	chi-square	γ_r (%)	a	chi-square	γ_r (%)	α	b	chi-square
SLC14	RC	7.8	5.918e5	0.0876	3.832e-4	0.0719	0.8014	1.328e-4	0.0644	2.5520	2.5660	6.295e-5
		15.6	8.200e5	0.1045	1.335e-3	0.0169	0.7898	1.992e-4	0.0765	3.0820	2.5711	1.919e-4
		31.2	1.175e6	0.1000	3.349e-4	0.0741	0.8210	7.909e-4	0.0356	0.9476	2.8067	4.986e-4
	TS	7.8	6.213e5	0.0680	2.297e-5	0.0767	1.1452	1.852e-6	0.0278	3.0341	4.0786	1.094e-6
		15.6	8.628e5	0.1094	8.992e-5	0.1037	0.9067	2.957e-5	0.0723	1.9080	2.7680	5.563e-6
		31.2	1.232e6	0.0649	2.192e-4	0.0720	1.3202	2.105e-6	0.0437	2.4400	4.3630	2.997e-5
SLC35	RC	13.2	6.897e5	0.0769	3.027e-4	0.0640	0.7958	1.695e-5	0.0670	2.4297	2.4638	6.825e-8
		26.4	1.370e6	0.0696	2.830e-4	0.0669	0.9522	2.185e-4	0.0438	2.0074	3.0837	1.312e-5
	TS	13.2	7.568e5	0.0737	1.233e-4	0.0640	0.8463	1.189e-5	0.0528	2.4193	2.6647	2.577e-6
		26.4	1.480e6	0.0787	9.096e-6	0.0783	0.9819	1.086e-5	0.0486	1.6063	2.8360	1.232e-5

Note: 1. Due to the technical program, the TS test was not performed on this sample
2. Shaded fields represent the best fit soil model

The modified hyperbolic model fit was the most commonly selected model for predicting the τ–γ relationships for Bonneville clay in this study. The Ramberg-Osgood model generally fit the T-θ relationship at high strains better than the other two models. However, the Ramberg-Osgood model fit the data poorly at strain levels close to the elastic threshold strain, γ_e^t. The hyperbolic model fit the T–θ relationship well at low to medium strain levels but typically fit the data poorly at high strain levels.

4.2.2 Development of Modulus Reduction Curve. The modulus reduction curve (G versus log γ), and normalized modulus reduction curve (G/G_{max} versus log γ) were developed from the τ–γ relationship that provided the best fit to the measured T-θ data. The modulus reduction curve and normalized modulus reduction curve are generated as continuous functions. They can be generated for over any range of strains. However, it is only rational to develop the curve for strain levels in the range where the T-θ relationship was measured. In this study, the modulus reduction curve was generated for each RC and TS test for the range of strain levels up to the strain level performed in each test which was corresponded to the maximum measured rotation, θ_{max} measured for each test. The equivalent radius approach was used to determine maximum measured strain, γ_{max}, corresponded to that value of θ_{max}. The γ_{max}, of each test is calculated from:

$$\gamma_{max} = R_{eq} \frac{\theta_{max} R}{L} \tag{3}$$

where R_{eq} = equivalent radius ratio
R = radius of soil specimen, and
L = length of soil specimen.

The parameter γ_r from the hyperbolic model was used to obtain a normalized rotation (θ_{max}/θ_r). Thus, the value of R_{eq} is obtained from the normalized R_{eq} curve based on shear modulus developed in Sasanakul (2005) and presented in Figure 8. The modulus reduction curve at strains above γ_{max} is uncertain.

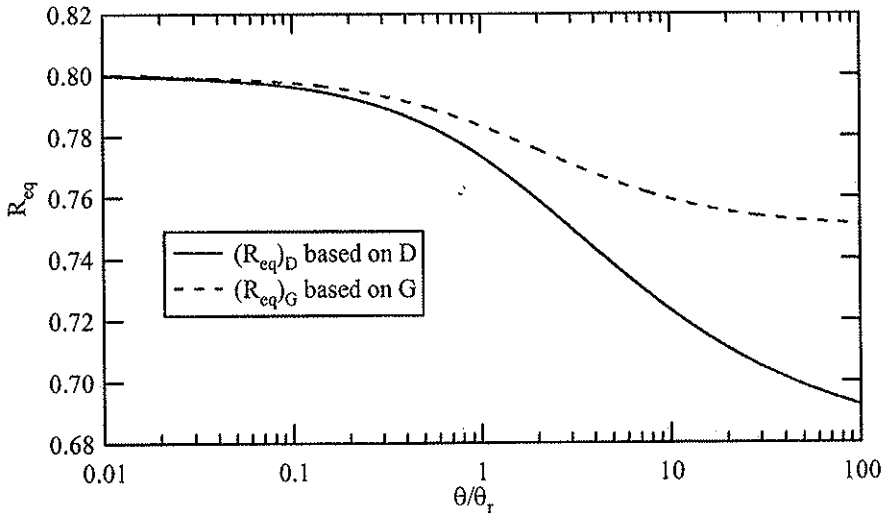

Figure 8 R_{eq} curves versus normalized rotation based on G and D (Sasanakul 2005)

The modulus reduction curve and normalized modulus reduction curve from RC and TS tests on each soil specimen are presented in Figures 9-15. The modulus reduction curves are plotted versus strain level up to the maximum measured strain. The curve was then extended to higher strains using the dashed lines.

The results from RC and TS test were compared for all soil specimens except for specimen PRV37. On this sample, only the RC test was performed. It should be noted that the shear moduli obtained in the TS test, were evaluated from the first cycle of the hysteresis loop. For all of the specimens except for specimen NBL24, the shear modulus from TS test is higher than the shear modulus from the RC test. The two differences between the RC and TS tests are the frequency and the number of loading cycles. The TS tests were performed at a frequency of 0.333 Hz for five cycles while the RC test was performed at resonant frequency with a high number of cycles. In general, the stiffness of a cohesive soil increases as the frequency increases. On the other hand, stiffness decreases as the number of cycles increases (Kim 1991). The lower values of shear modulus in RC test maybe explained by the effects of cyclic degradation outweighing the frequency effects.

The effect of confining pressure can be investigated using the normalized modulus reduction curves. In Figures 9-15, the normalized modulus reduction curves show small effects of confining pressure with the curves falling in a very narrow band especially below the threshold strain γ_e^t.

4.2.3 Development of Damping Curve. Material damping of the soil was determined using the half power bandwidth method and the free vibration decay method for the RC tests, and hysteretic damping for TS tests. The damping, D, was measured with an associated θ for each method. To develop damping curves, the modified R_{eq} approach presented in Sasanakul (2005) was used. The R_{eq} for damping can be obtained for any given θ using the curve presented in Figure8, if the hyperbolic reference strain, γ_r is known.

Procedures for developing damping curves are as follows. (1) Determine the value of γ_r from hyperbolic model using the stress integration approach. (2) Calculate normalized quantity θ/θ_r where θ_r is calculated using $\theta_r = \frac{\gamma_r L}{R}$. (3) Determine the value of R_{eq} from Figure 8. (4) Calculate γ for a given θ using the R_{eq} value. Figure 16 shows an example of the R_{eq} values used to develop the damping curve for the TS test on sample PRV93.

In this study, the half power bandwidth method was used in the RC test for determining damping of soil in its linear range (D_{min}). The free vibration decay method was used to determine the damping at high strains in the RC tests. Free vibration decay tests were only performed on soil specimens obtained from Logan and near Salt Lake City Airport. Figures 17-19 shows the material damping curves for specimens from Provo and Nibley. The high strain damping of specimens from Provo and Nibley were obtained only from the TS test. The damping for specimen PRV37 is not presented because the TS test was not performed on this specimen.

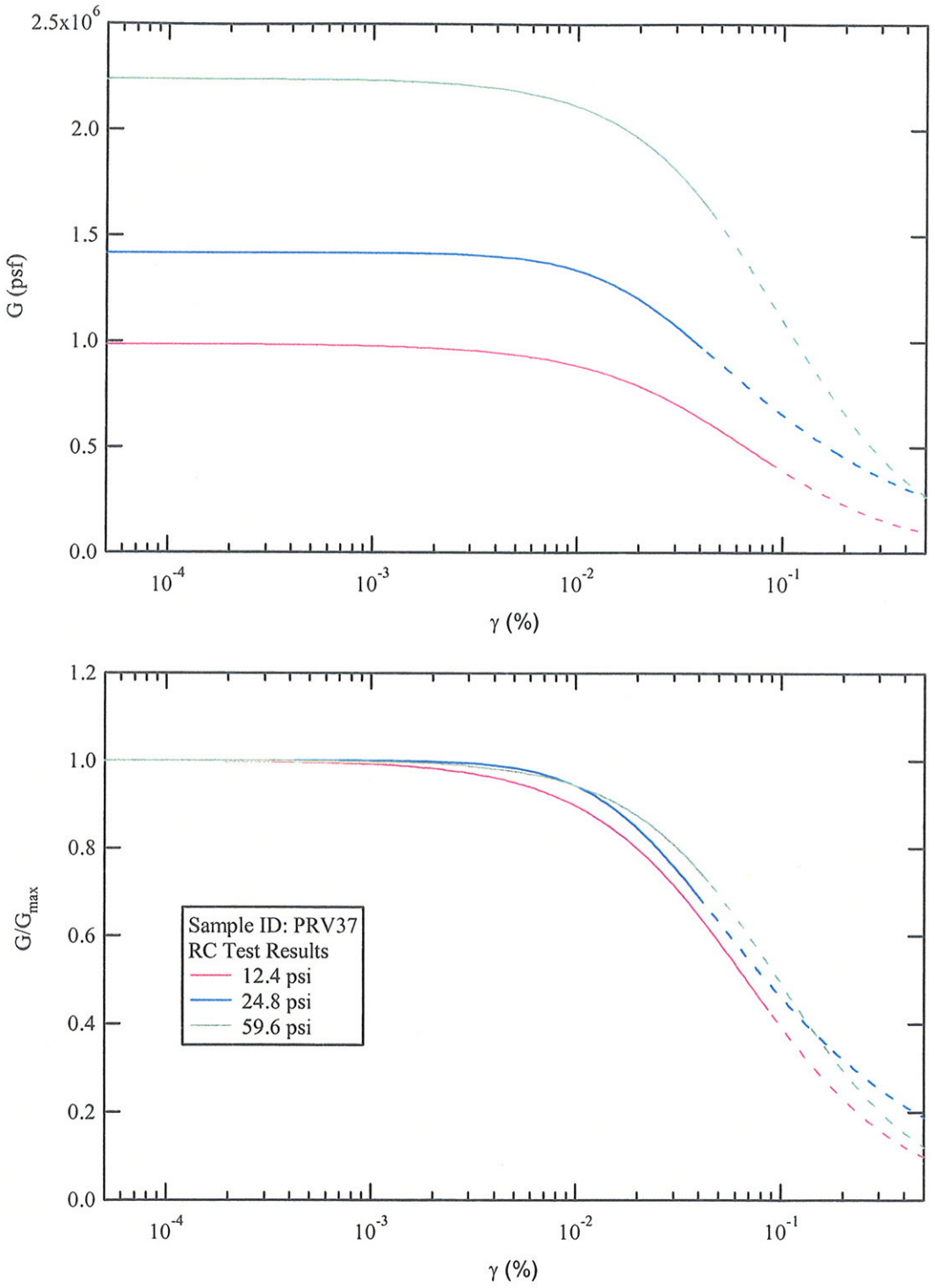

Figure 9 Modulus reduction curves and normalized modulus reduction curves measured at various confining pressures for soil specimen PRV37 near the Provo River at a depth of 37 ft

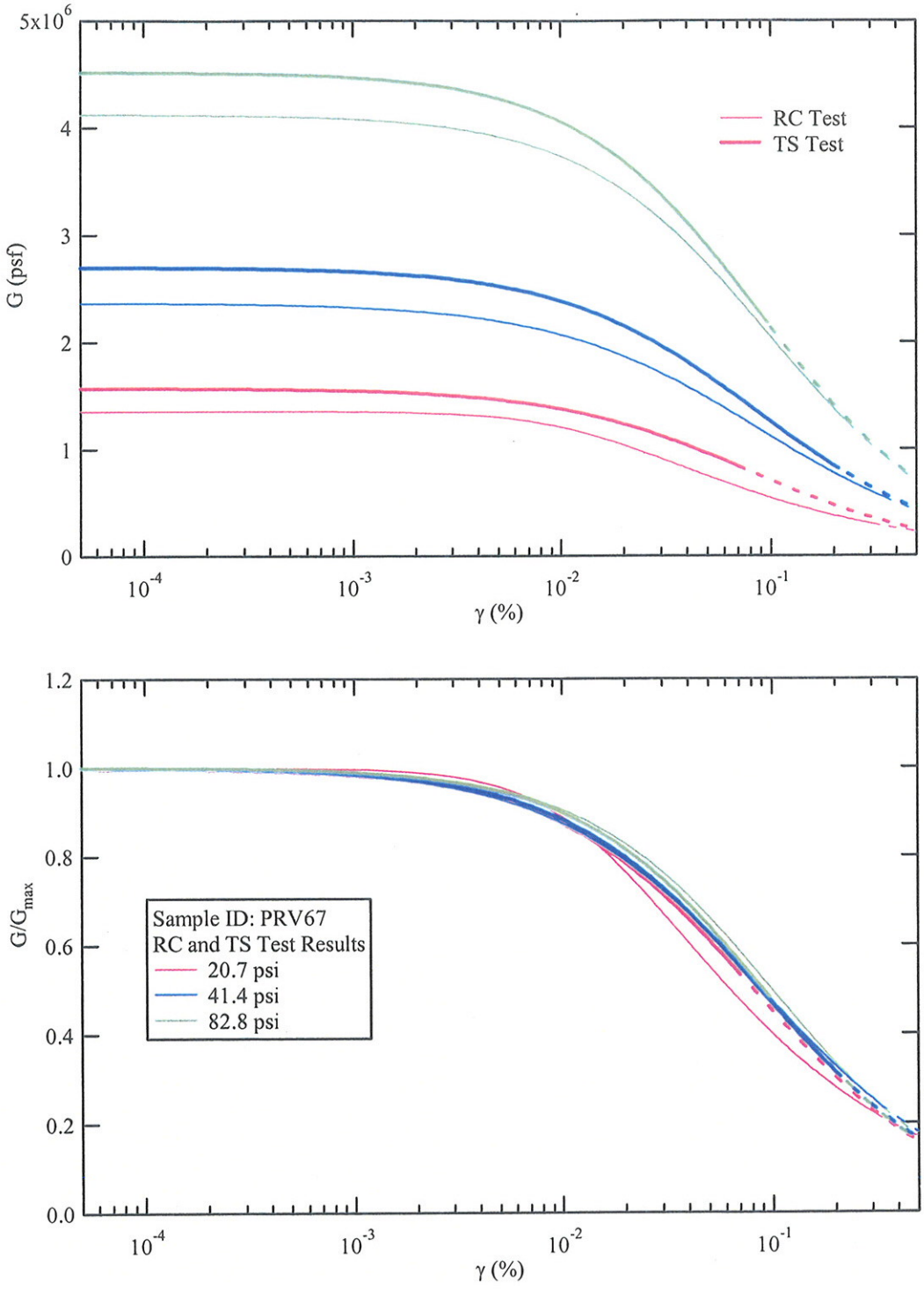

Figure 10 Modulus reduction curves and normalized modulus reduction curves measured at various confining pressures for soil specimen PRV67 near the Provo River at a depth of 67 ft

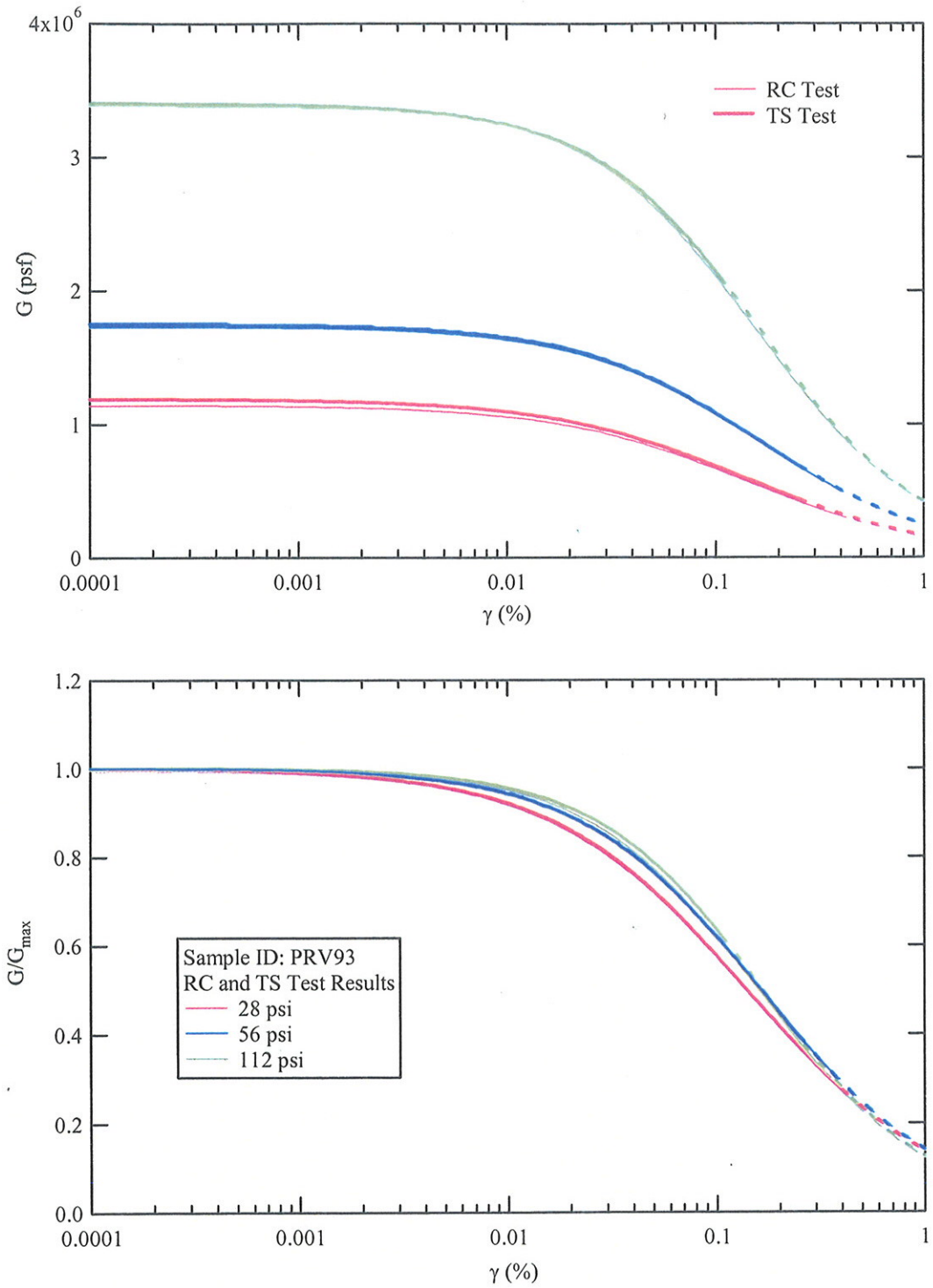

Figure 11 Modulus reduction curves and normalized modulus reduction curves measured at various confining pressures for soil specimen PRV93 near the Provo River at a depth of 93 ft

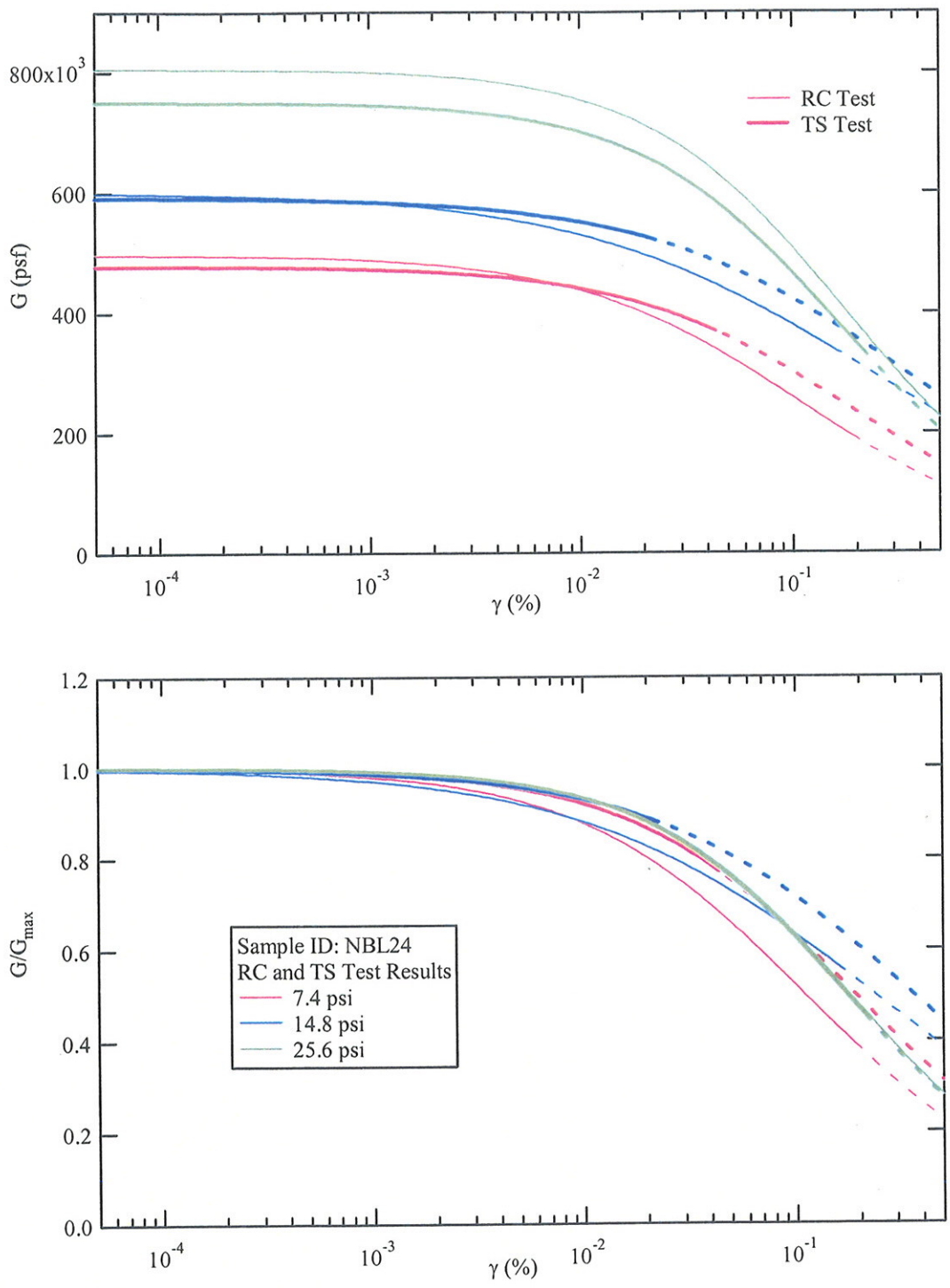

Figure 12 Modulus reduction curves and normalized modulus reduction curves measured at various confining pressures for soil specimen NBL24 at Nibley at a depth of 24 ft

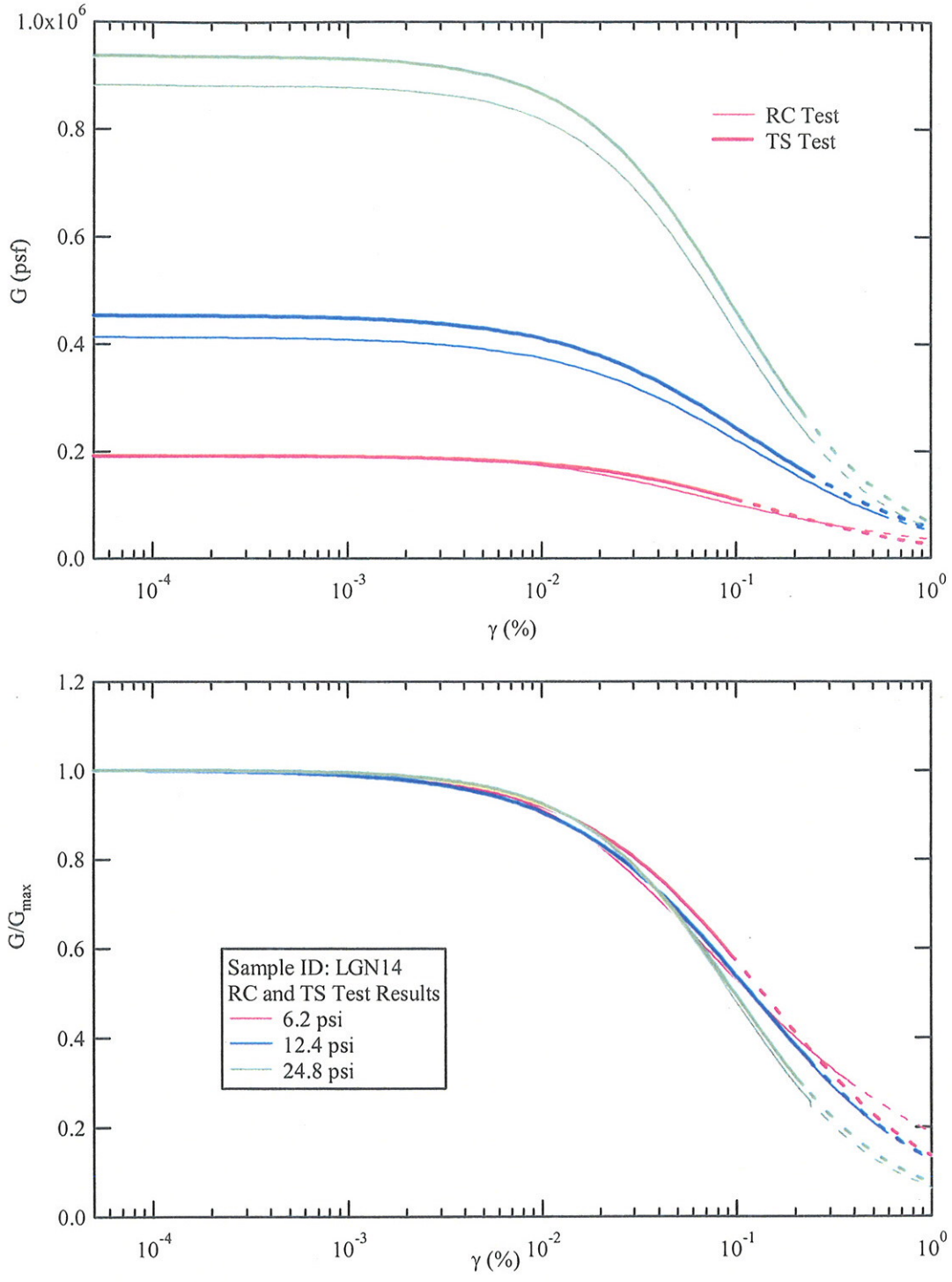

Figure 13 Modulus reduction curves and normalized modulus reduction curves measured at various confining pressures for soil specimen LGN14 at Logan at a depth of 14 ft

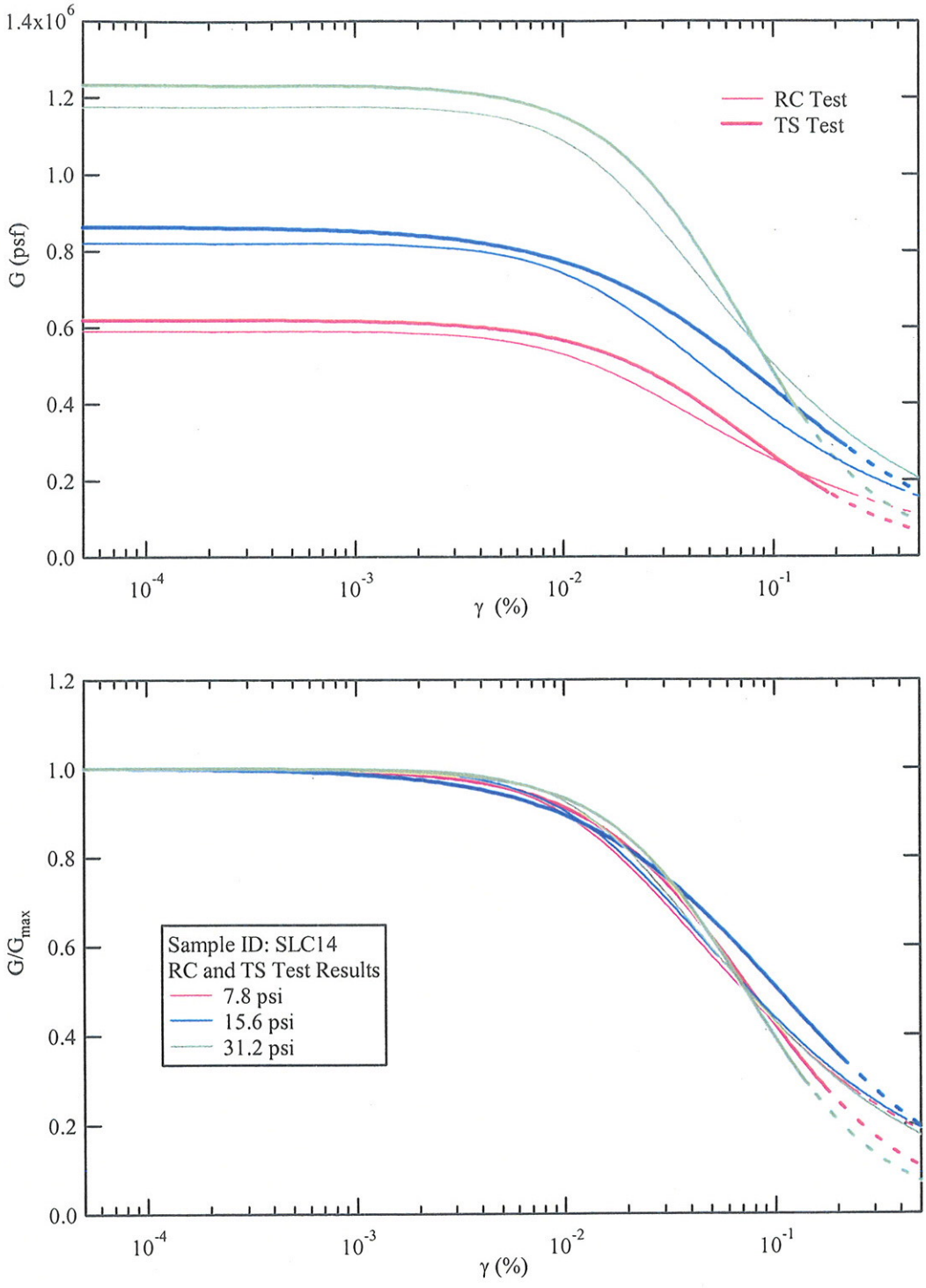

Figure 14 Modulus reduction curves and normalized modulus reduction curves measured at various confining pressures for soil specimen SLC14 near Salt Lake City Airport at a depth of 14 ft

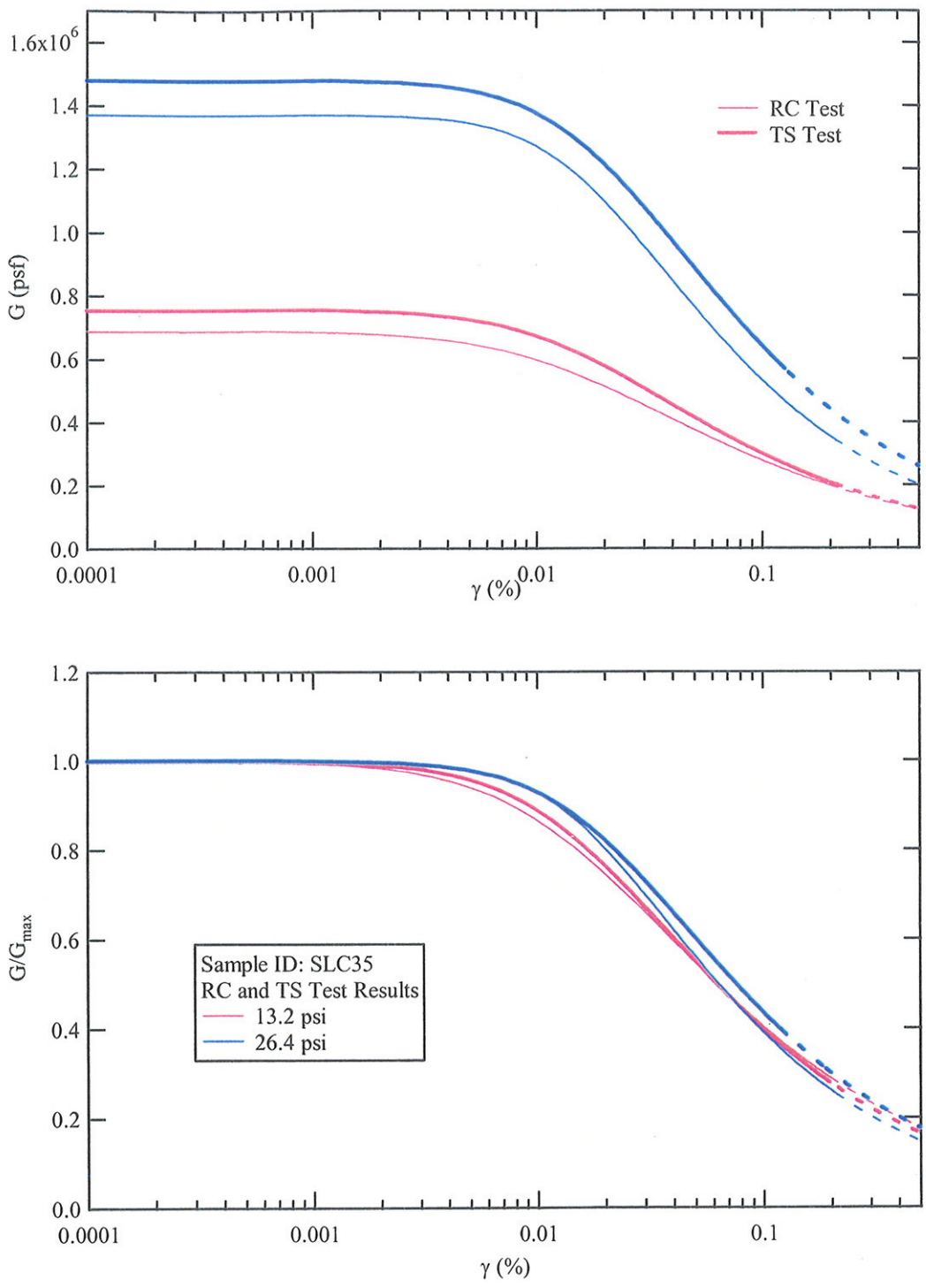

Figure 15 Modulus reduction curves and normalized modulus reduction curves measured at various confining pressures for soil specimen SLC35 near Salt Lake City Airport at a depth of 35 ft

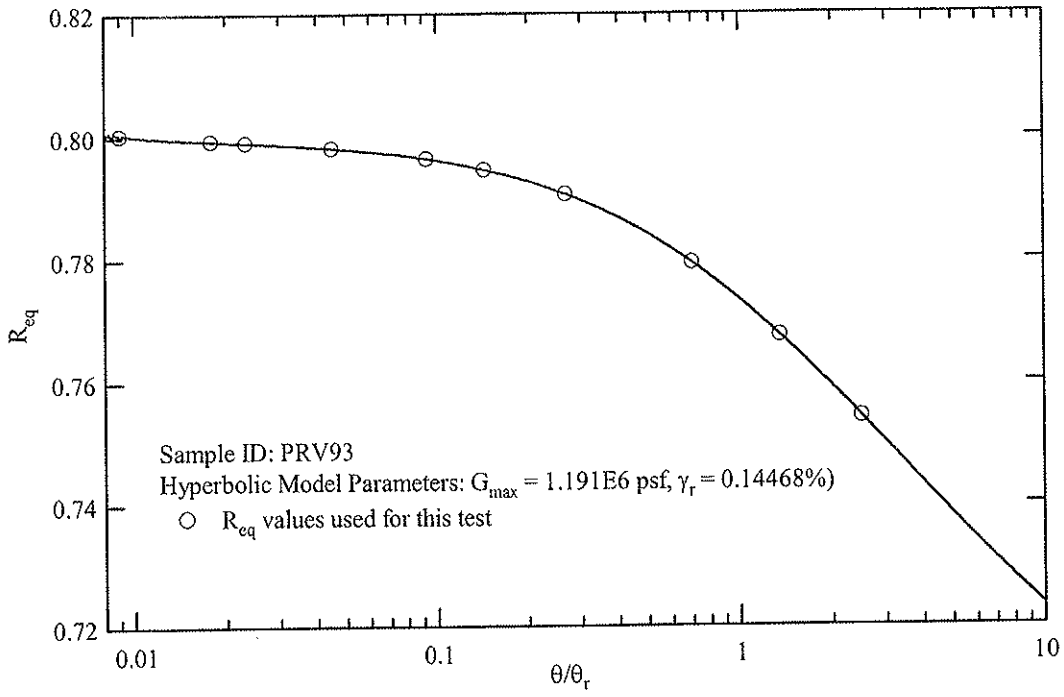

Figure 16 Example for the evaluation of R_{eq} values for generating material damping curves for specimen PRV93

Figures 20-22 shows a comparison of material damping from RC and TS tests for specimens obtained from Logan and near the Salt Lake City Airport. The D_{min} obtained from RC and TS tests match well. However, the high strain damping measured in RC tests is higher than the damping measured in the TS tests. Typically, material damping for cohesive soil is independent of number of cycles but is significantly effect by the frequency (Kim, 1991). The RC and TS tests are performed at different frequencies. In the RC test, damping is measured at resonant frequency (above 10 Hz for this study) while the damping in the TS tests was measured at 0.333 Hz for this study.

Typically, the damping curve is not presented in terms of a normalized quantity. The effect of confining pressure can be observed from the typical damping curves as shown in Figures 17-22. In general, the damping value decreases as the confining pressure increases. In this study, the confining pressure has a very small effect on the damping of Bonneville clay. In most cases, the damping values measured at different confining pressures at the same strain level are similar. An example of this is specimen PRV93 presented in Figure 18.

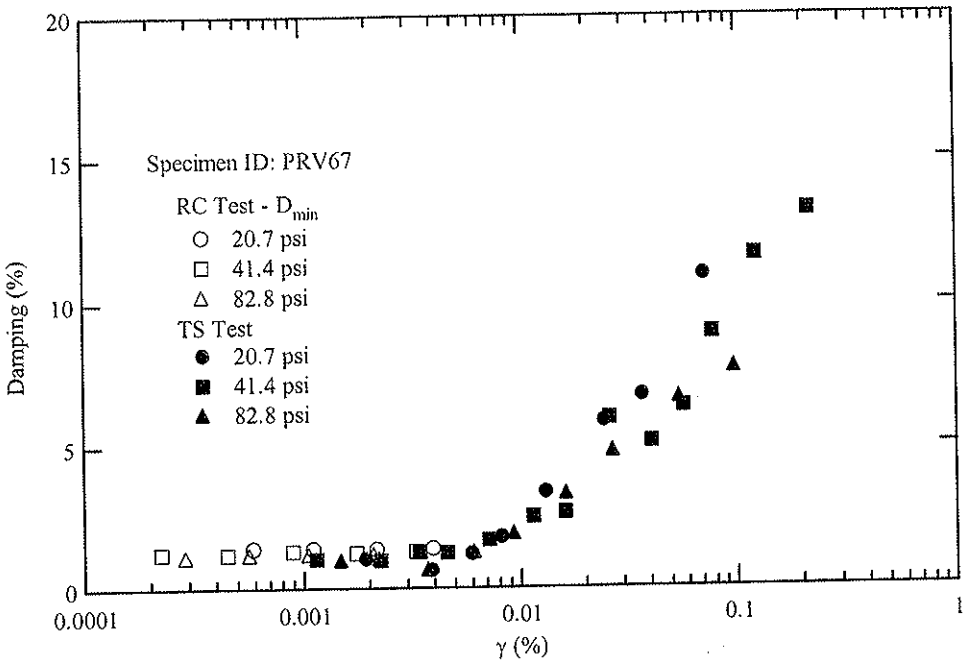

Figure 17 Damping curves measured on soil specimen PRV67 obtained near the Provo River at a depth of 67 ft

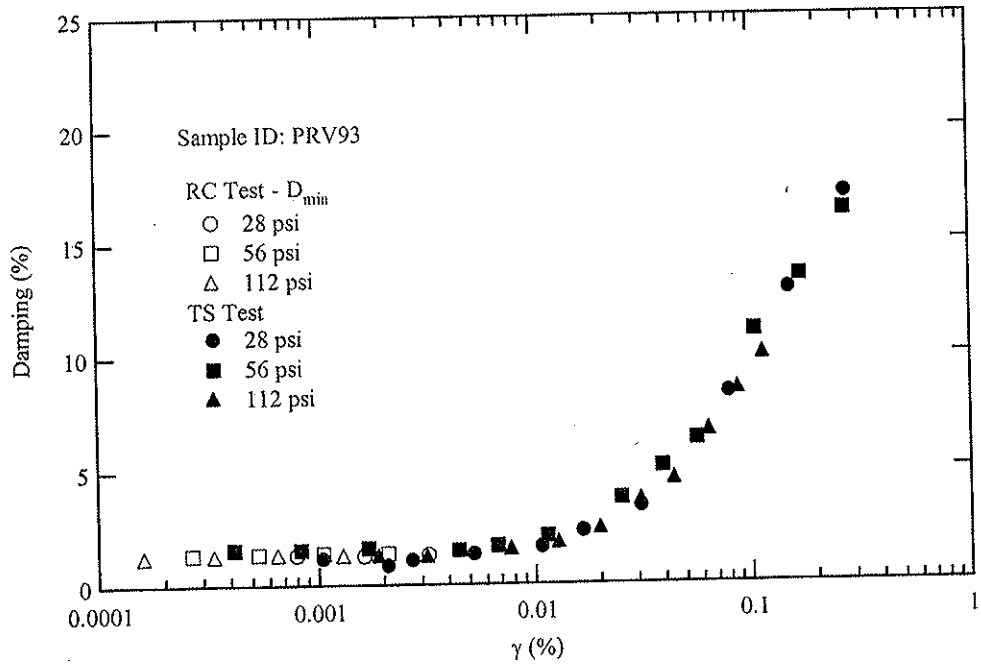

Figure 18 Damping curves measured on soil specimen PRV93 obtained near the Provo River at a depth of 93 ft

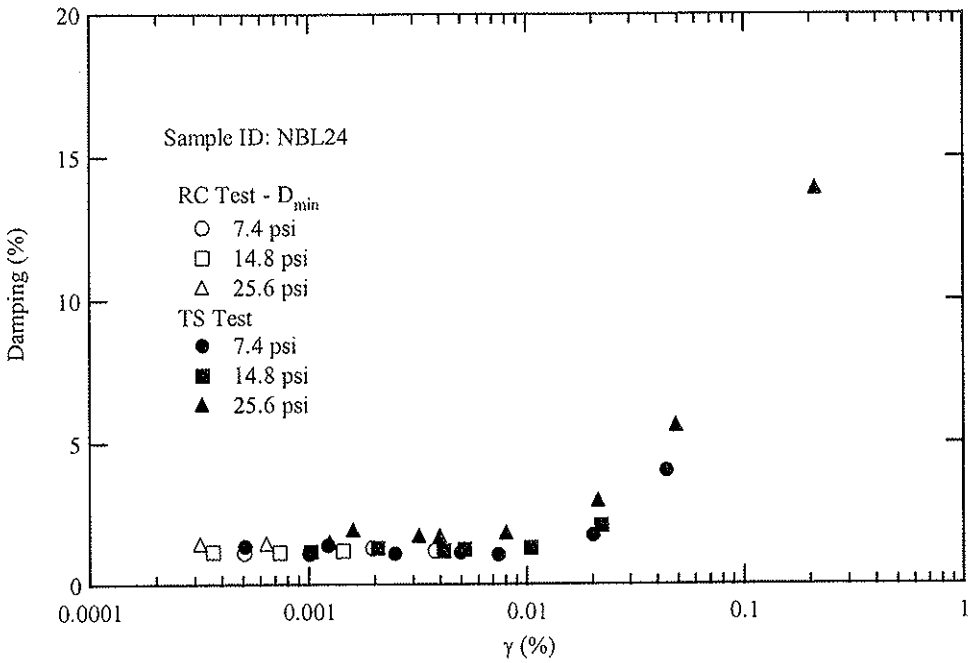

Figure 19 Damping curves measured on soil specimen NBL24 obtained from Nibley at a depth of 24 ft

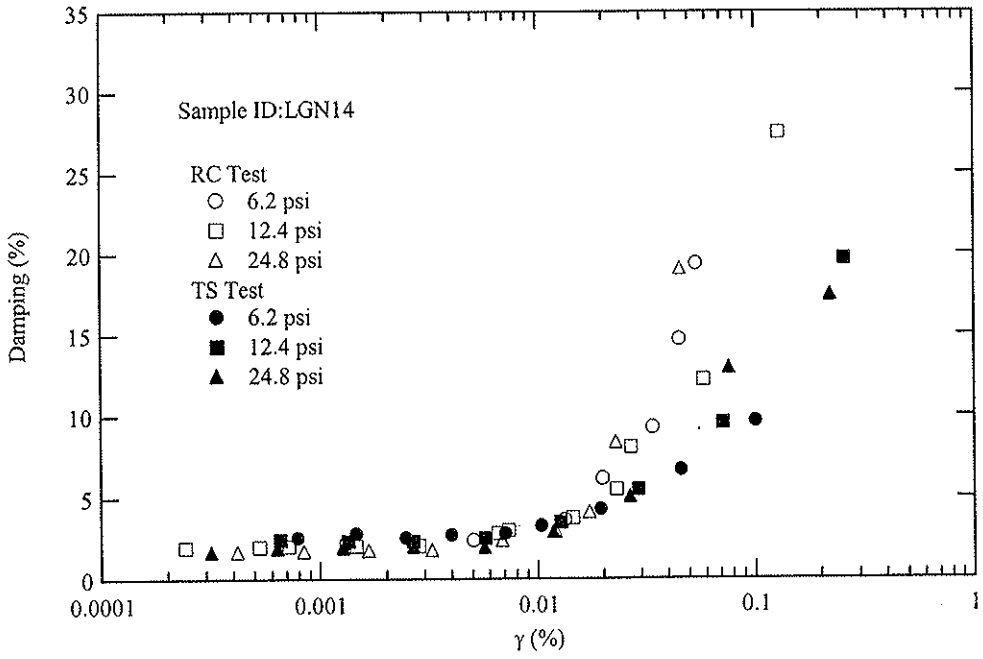

Figure 20 Damping curves measured on soil specimen LGN14 obtained from Logan at a depth of 14 ft

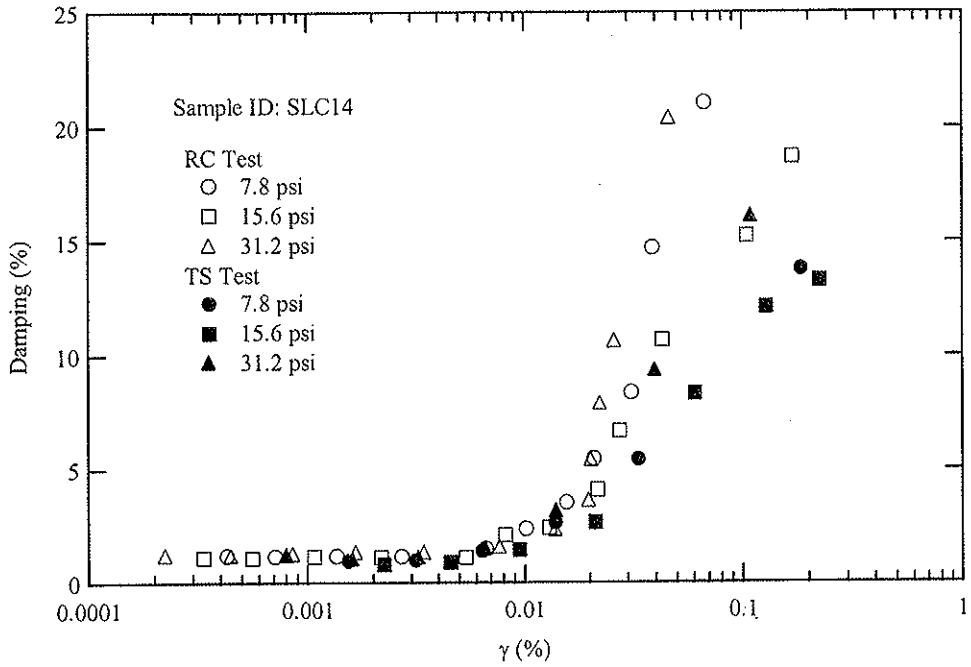

Figure 21 Damping curves measured on soil specimen SLC14 obtained near Salt Lake City Airport at a depth of 14 ft

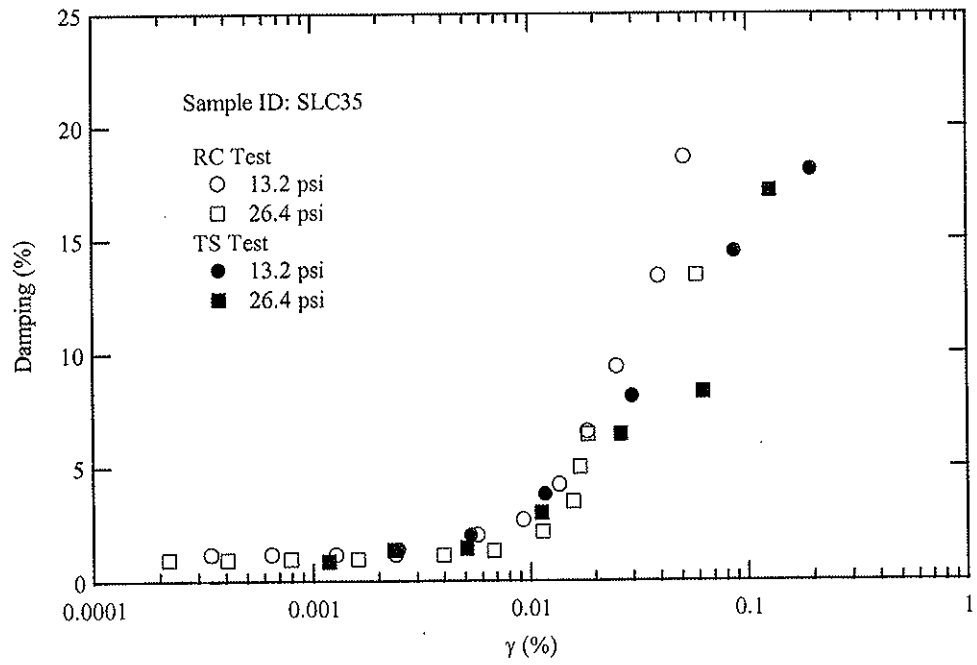

Figure 9.22 Damping curves measured on soil specimen SLC35 obtained near Salt Lake City Airport at a depth of 35 ft

5 DISCUSSION ON FACTORS AFFECTING MODULUS REDUCTION AND DAMPING CURVES

This section contains a discussion of the effects of plasticity index and confining pressure on the normalized modulus reduction and damping curves. The normalized modulus reduction curves and damping curves are compared with generic curves used in practice for a given plasticity index and confining pressure.

5.1 Plasticity Index Effect

An important soil property affecting the nonlinear stress-strain behavior of clay is plasticity index (PI). The seven Bonnville clay specimens used in this study have PI's ranging from 2 to 34 as shown in Table 2. The effect of PI can be evaluated using normalized modulus reduction curves for all soil specimens at their in situ mean effective confining pressure presented in Figure 23.

The normalized modulus reduction curves presented in Figure 23 were determined from RC and TS tests. Soil specimens used in this study can be divided into four groups: samples with PI's of 34, samples with PI's of 17-20, samples with PI's of 10-11, and samples with PI's of 2. In general, soil behaves more linearly (the elastic threshold strain, γ_e^t, increases) as the PI increases. This general trend of PI with soil linearity is not clearly observed in the RC test results. For the TS test results, the samples with PI of 34 behave more linear than the samples with PI's of 10-17. An outlier was observed in sample with a PI of 11 that behaves as linearly as the samples with a PI of 34. The sample with a PI of 2 was expected to behave the most nonlinearly but, the results show that this sample behaves similarly to the samples with PI's of 10-20. This might be because this sample has the interbeded layers of silt and clay. The clay layers may have more effect on damping than the silt layers.

The variation of damping with PI for the Bonneville clay tested in this study is presented in Figure 24. In general, the damping decreases as PI increases. The measured damping in TS test on specimen SLC35 with PI of 2 has the highest damping value. In the TS tests, the damping in specimens LGN14 and NBL24 with PI's of 34 show the lowest values of damping. Therefore, the damping behavior of Bonneville clay is typical of cohesive soils.

Empirical curves used to estimate modulus reduction and damping curves based upon PI where compared with the results from RC and TS tests on Bonneville clay. The empirical curves used are curves by Sun et al. (1988), Vucetic and Dobry (1991), and Darendeli (2001).

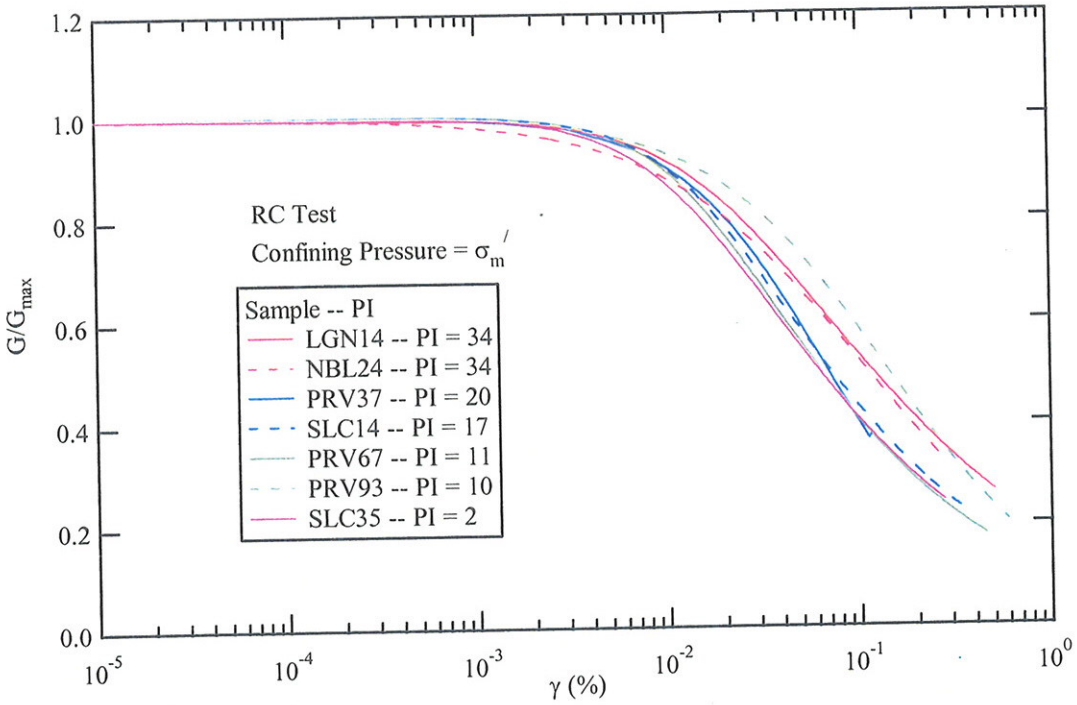

a) RC test results

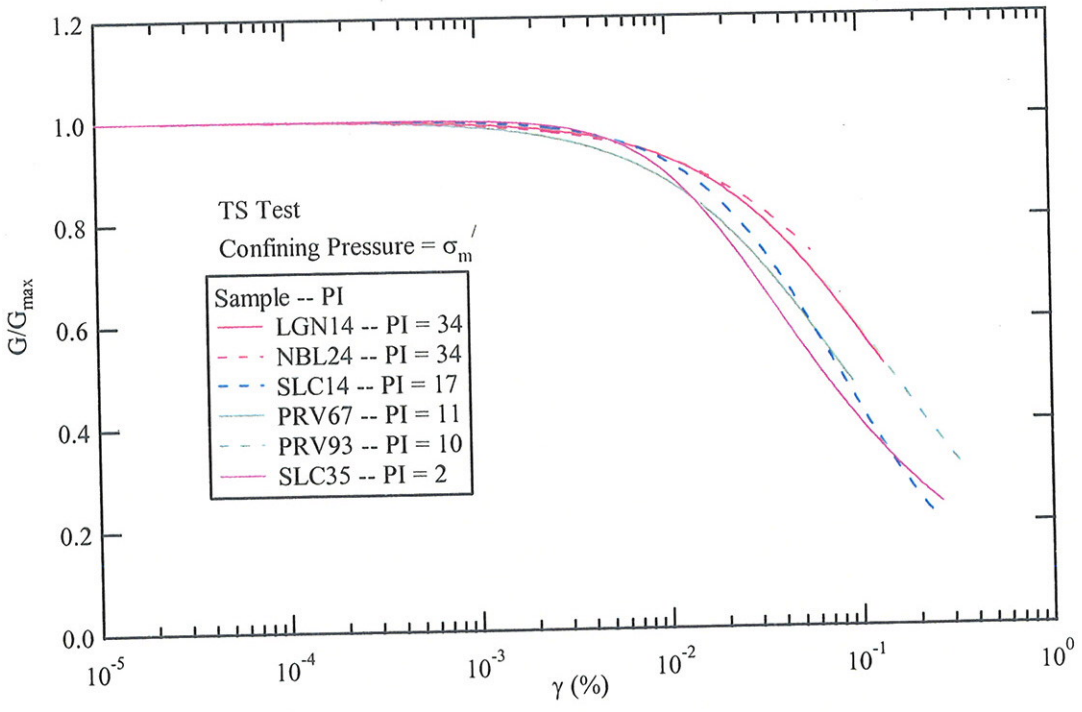

b) TS test results

Figure 23 Variation of normalized modulus reduction curves with PI for RC and TS tests on Bonneville clay

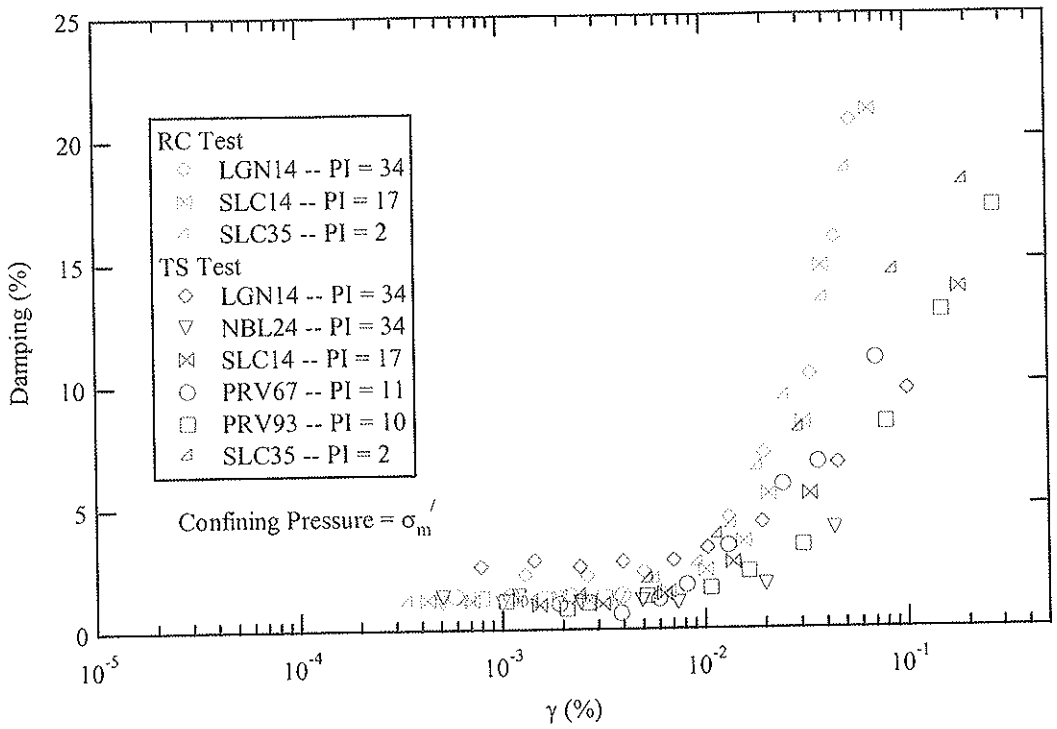

Figure 24 Variation of damping with PI for RC and TS tests on Bonneville clay

Sun et al. (1988) proposed empirical modulus reduction and damping curves for clays with different ranges of PI's. Figure 25 and 26 show the comparison for the curves measured in this study and the curves proposed by Sun et al. (1988). In Figure 25, three empirical curves are plotted for PI ranges of 5-10, 10-20, and 20-40. Bonneville clay specimens with PI's of 2-20 plot close to the Sun et al (1988) curve for a PI range of 10-20. The modulus reduction curves for samples with PI of 34 are in reasonably agreement with the Sun et al curve for a PI range of 20-40. The empirical curve for a PI range of 5-10 underestimates the measured modulus for the soil specimen with a PI of 2.

Sun et al. (1988) proposed the empirical damping curves with no correlation to PI as shown in Figure 26. The damping curve of Bonneville clay from TS tests plot close to the average curve at medium strains and close to the upper bound at high strains. While the small strain damping curve plots closer to the lower bound curve. However, these empirical damping curves span such a wide band that they are of little practical value.

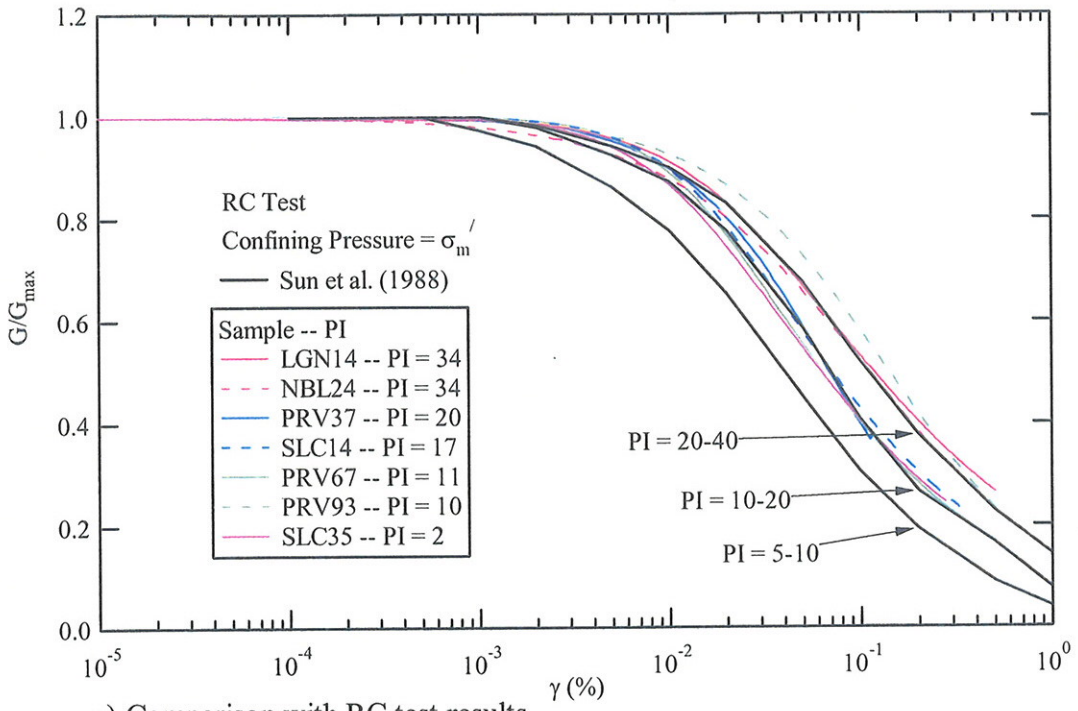

a) Comparison with RC test results

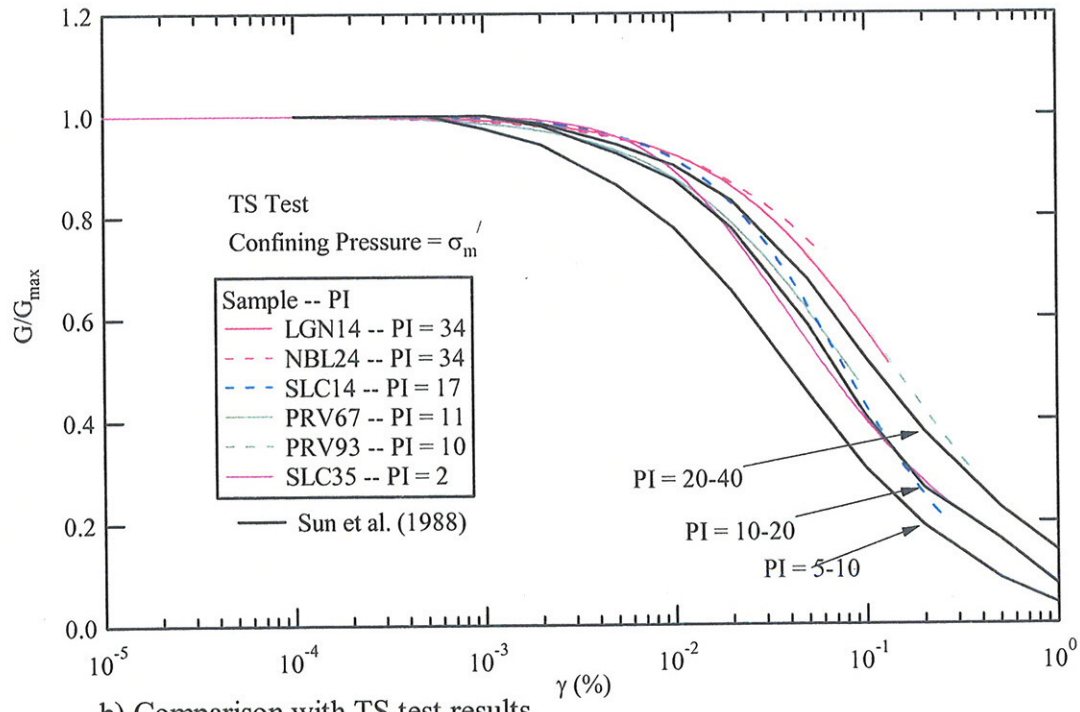

b) Comparison with TS test results

Figure 25 Comparison of normalized modulus reduction curves of Bonneville clay with empirical curves proposed by Sun et al. (1988)

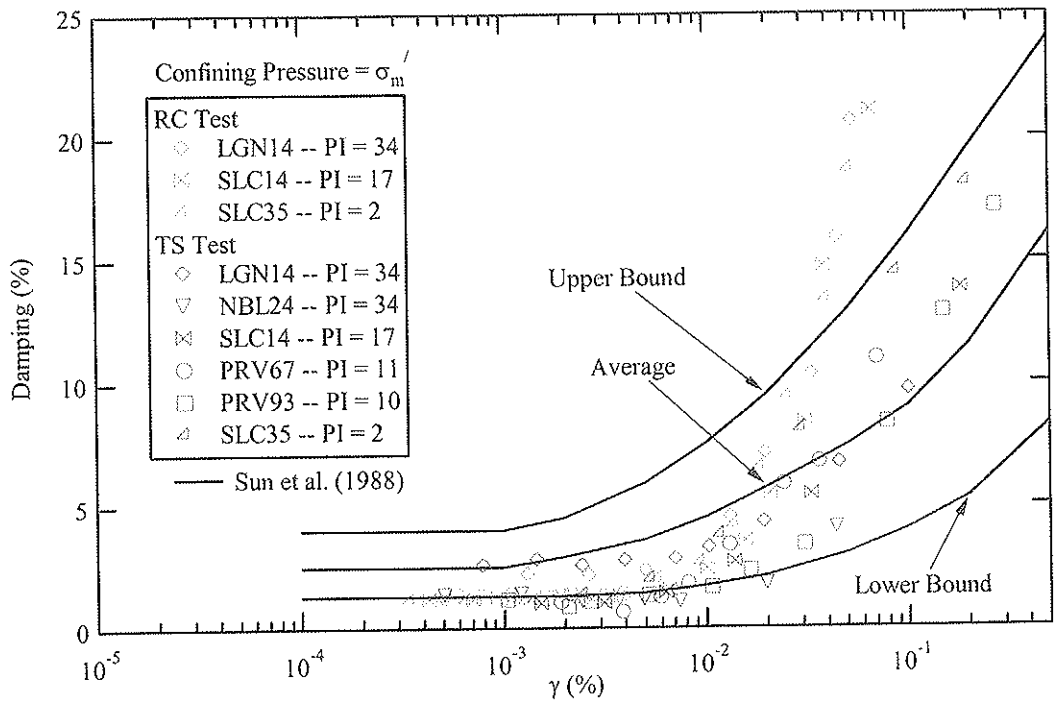

Figure 26 Comparison of damping curves of Bonneville clay with empirical curves proposed by Sun et al. (1988)

Comparisons of modulus reduction curves and damping curves to the empirical curves proposed by Vucetic and Dobry (1991) are presented in Figures 27-28. The Vucetic and Dobry (1991) curves for PI of 2, 10, 20, and 34 were generated by interpolation from their original proposed curves. In Figure 27, the Vucetic and Dobry (1991) modulus reduction curve for PI of 34 shows good agreement with the curves of Bonneville clays with the same PI value. The Vucetic and Dobry (1991) curves for PI of 2 and 10 exhibit more nonlinearity than the actual behavior of Bonneville clay at the same values of PI.

Damping curves proposed by Vucetic and Dobry (1991) show higher values of damping at medium strain levels (10^{-3}-10^{-2}%) than the damping curves for Bonneville clay presented in Figure 28. The Vucetic and Dobry (1991) damping curves also show a more pronounced effect of PI than was measured on the Bonneville clay. The Vucetic and Dobry (1991) damping curves have been left undefined at low strains. At high strains, the Vucetic and Dobry (1991) damping curves underestimates the Bonneville clay damping curves. The measured damping for the soil sample with a PI of 2 matches well with the Vucetic and Dobry (1991) curve for a PI of 2 at strains above 0.1%.

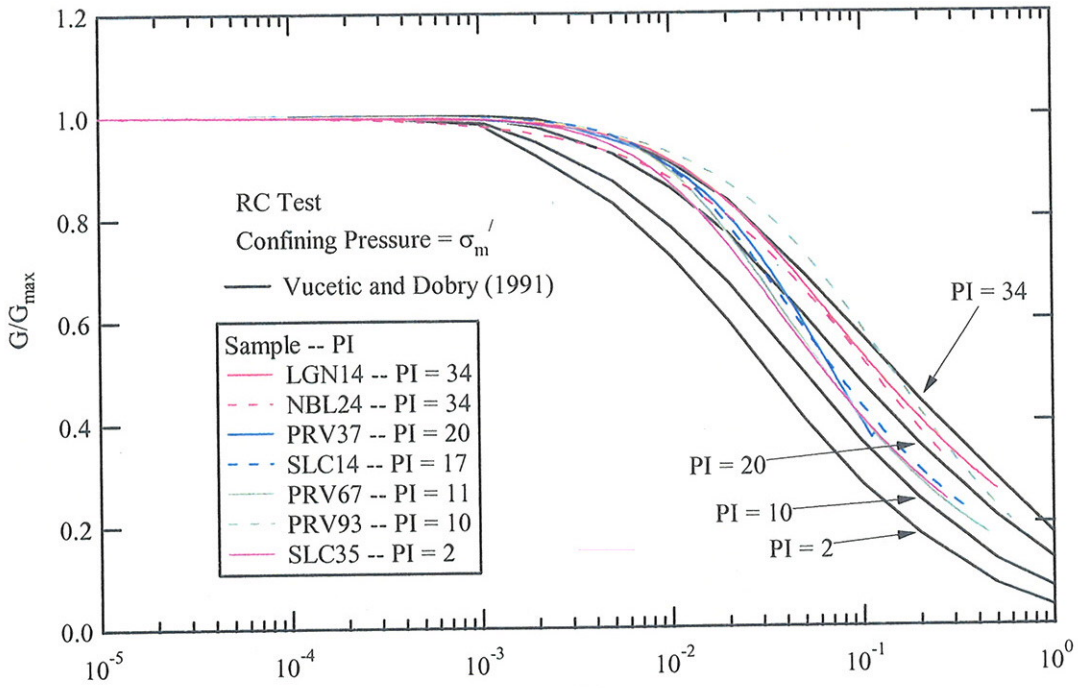

a) Comparison with RC test results γ (%)

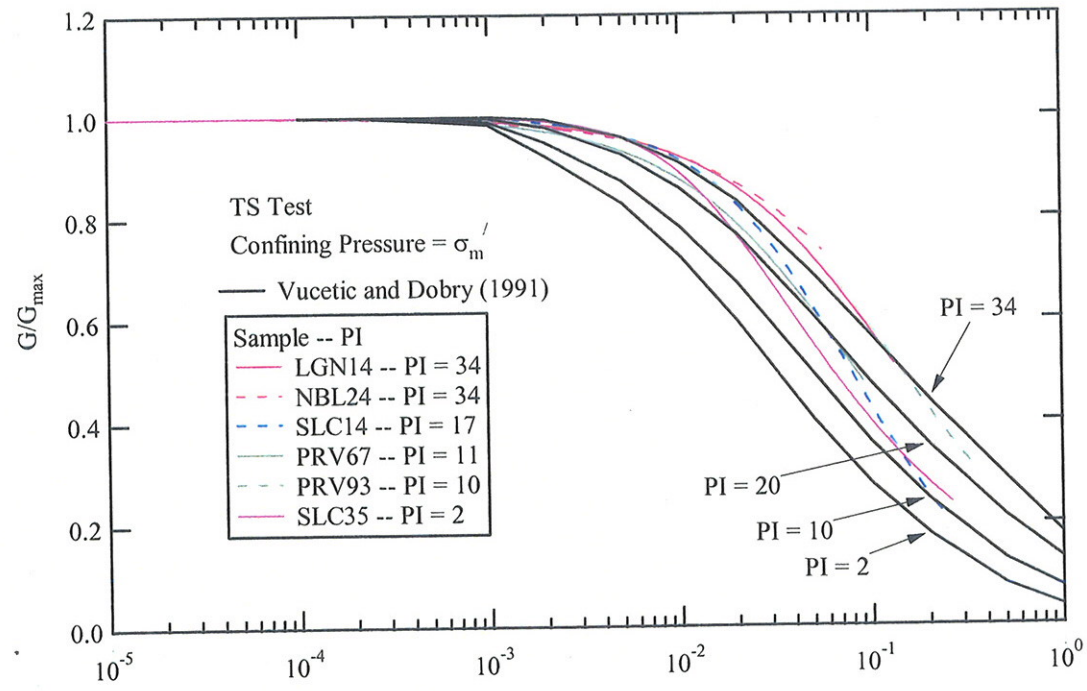

b) Comparison with TS test results γ (%)

Figure 27 Comparison of normalized modulus reduction curves of Bonneville clay with empirical curves proposed by Vucetic and Dobry (1991)

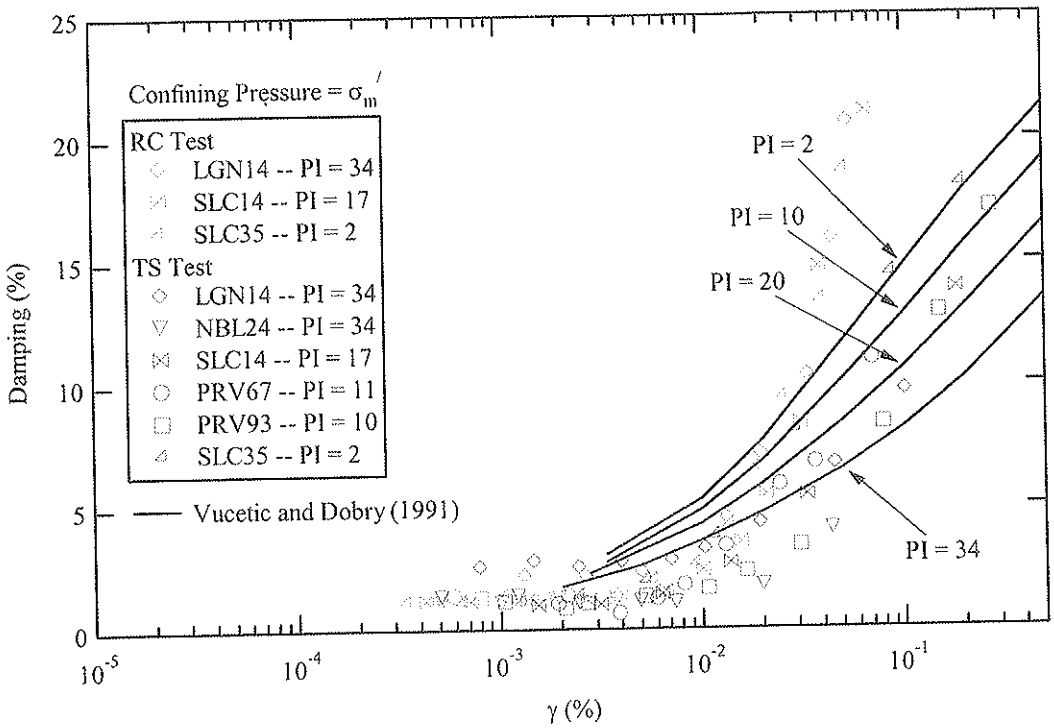

Figure 28 Comparison of damping curves for Bonneville clay with empirical curves proposed by Vucetic and Dobry (1991)

Darendeli (2001) proposed a model to predict the modulus reduction curves and damping curves accounting for the effect of PI, confining pressure, OCR, frequency (freq), and number of cycles (N). The modulus reduction curves and damping curves were generated using the proposed model by Darendeli (2001) for PI values of 2, 10, 20, and 34 with an OCR = 1, σ_m' = 1 atm, freq = 0.333 Hz, and N = 5 cycles. The Darendeli (2001) curves were compared with Bonneville clay curves in Figures 29-30.

The Darendeli (2001) modulus reduction curves show a smaller PI effect than the other empirical curves. In Figure 29, all of the Darendeli (2001) curves for different PI plot below the curve for Bonneville clay. This indicates that Bonneville clay behaves more linearly than predicted by the Darendeli (2001). It is interesting to note that the width of the band for effect of PI value of of 2 up to 34 predicted by Darendeli (2001) is close to the bandwidth of the measured curves.

Damping curves proposed by Darendeli (2001) are compared to the measured damping in Figure 30. Again, the damping curves proposed by Darendeli (2001) shows narrow band of PI effect. Damping from RC test was higher than that predicted damping by Darendeli (2001). However, the damping from TS tests matches the Darendel (2001) damping curve at high strains. The Darendeli (2001) damping curve slightly overestimates the damping at medium strains. This is consistent with the more linear behavior of Bonneville clay. The Darrendeli (2001) damping curve for a PI of 2 underpredicts the damping of the Bonneville clay at high strains.

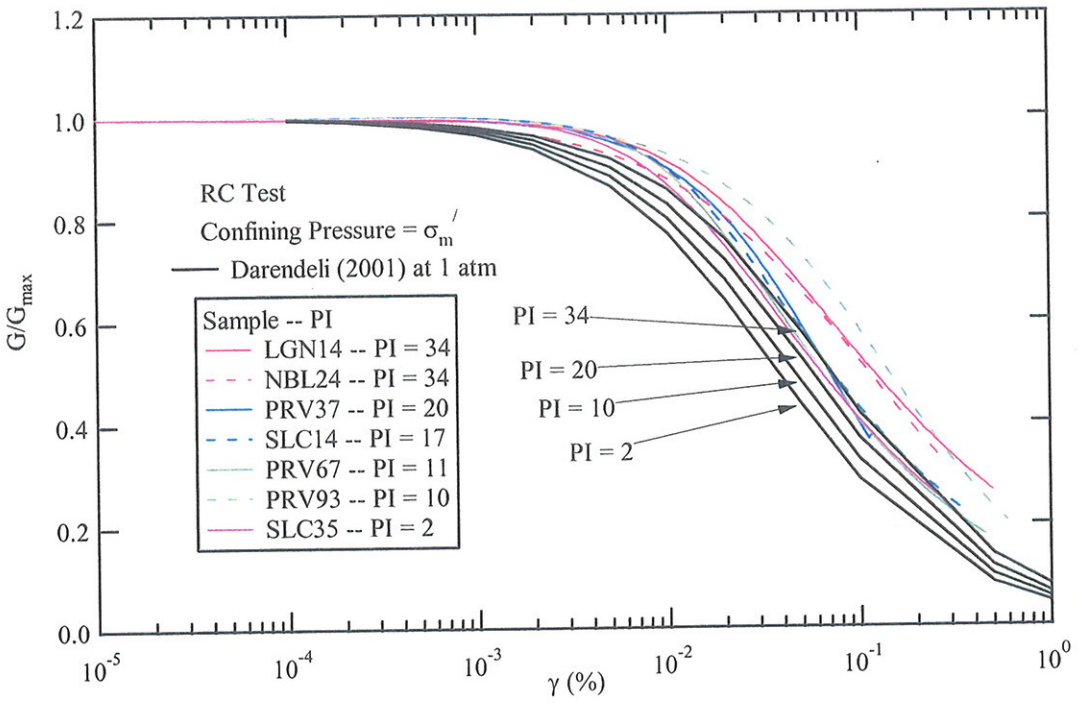

a) Comparison with RC test results

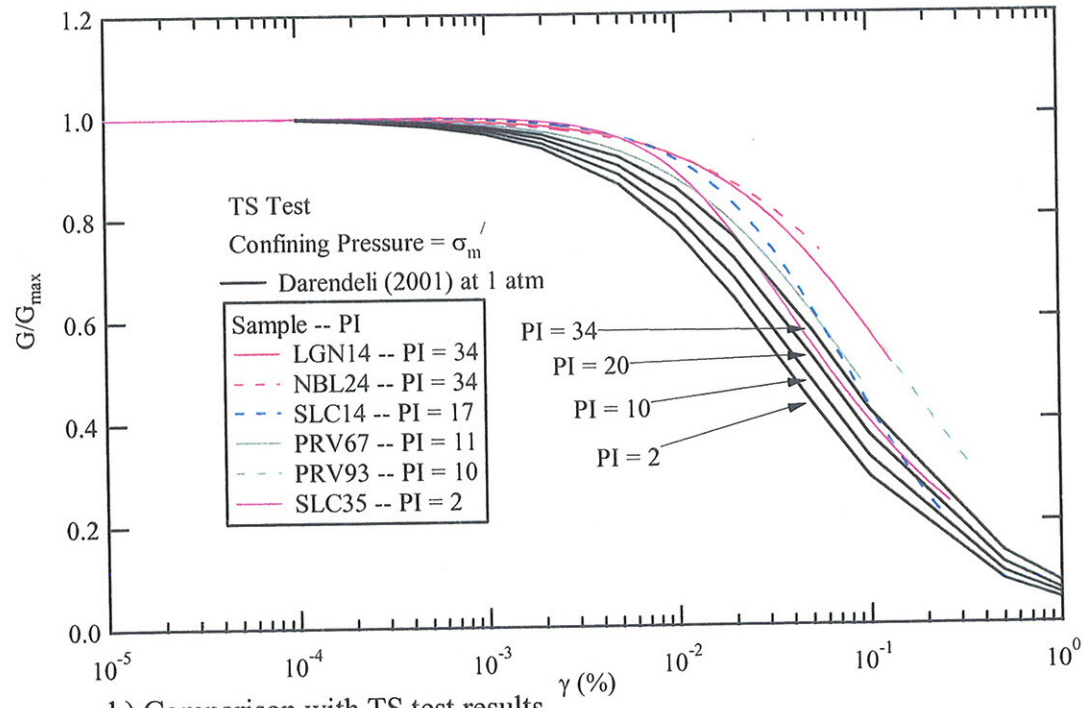

b) Comparison with TS test results

Figure 29 Comparison of normalized modulus reduction curves of Bonneville clay with empirical curves proposed by Darendeli (2001)

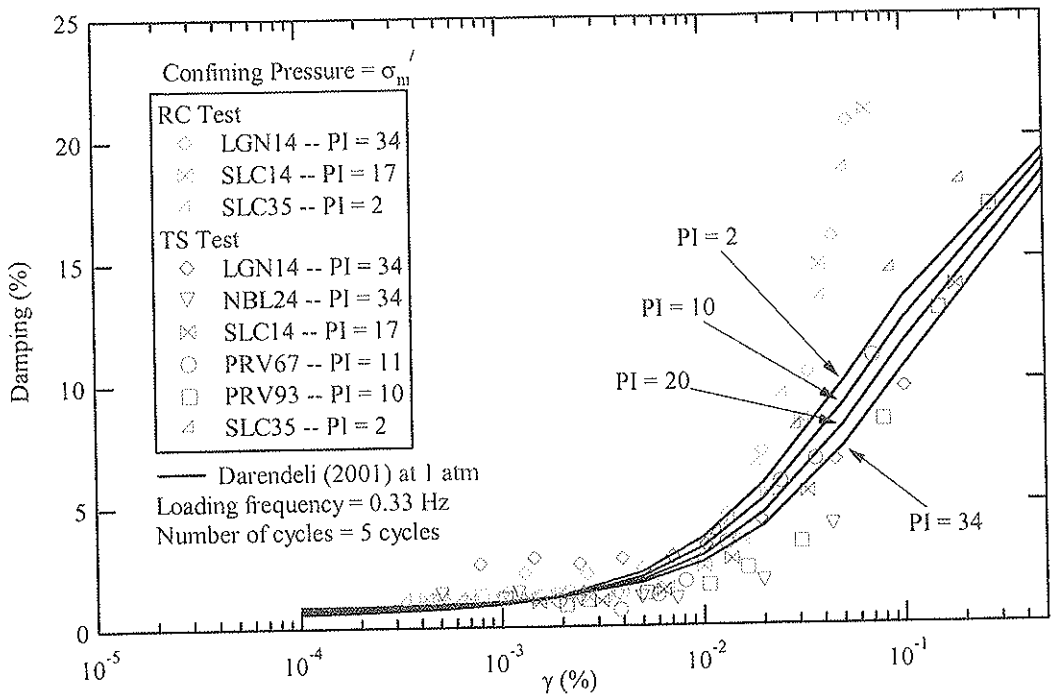

Figure 9.30 Comparison of damping curves for Bonneville clay with empirical curves proposed by Darendeli (2001)

5.2 Confining Pressure Effect

In this section, the effects of confining pressure on the modulus reduction curves and damping curves for Bonneville clay is compared with the empirical curves developed by Darendeli (2001). The empirical curves are compared with the results from TS tests on soil specimen PRV93. Three different confining pressures were applied to this specimens during testing. The sample PRV93 was confined at mean effective stresses of 28, 56, and 112 psi. The modulus reduction and damping curves of the specimen PRV93 are presented in Figures 11 and 18, respectively.

The normalized reduction and damping curves for sample PRV93 are compared with the Darendeli (2001) empirical curves presented in Figure 31. The normalized reduction curve becomes more linear as the confining pressure increases. Damping curves of specimen PRV93 shows a very small effect of the confining pressure.

The Darendeli (2001) curves in Figure 31 were regenerated for the same confining pressure at which each specimen was subjected to in the RC and TS tests. In Figure 31, the measured normalized modulus reduction curve for sample PRV93 plots above the predicted curves. Less effect of confining pressure is seen in the normalized reduction curves of PRV93 than that predicted by the Darendeli (2001). For damping, the Darendeli (2001) curve plots above the measured curve at medium strains. With the normalized modulus reduction curve, the effect of confining pressure in damping for PRV93 is less than that predicted by Darendeli (2001).

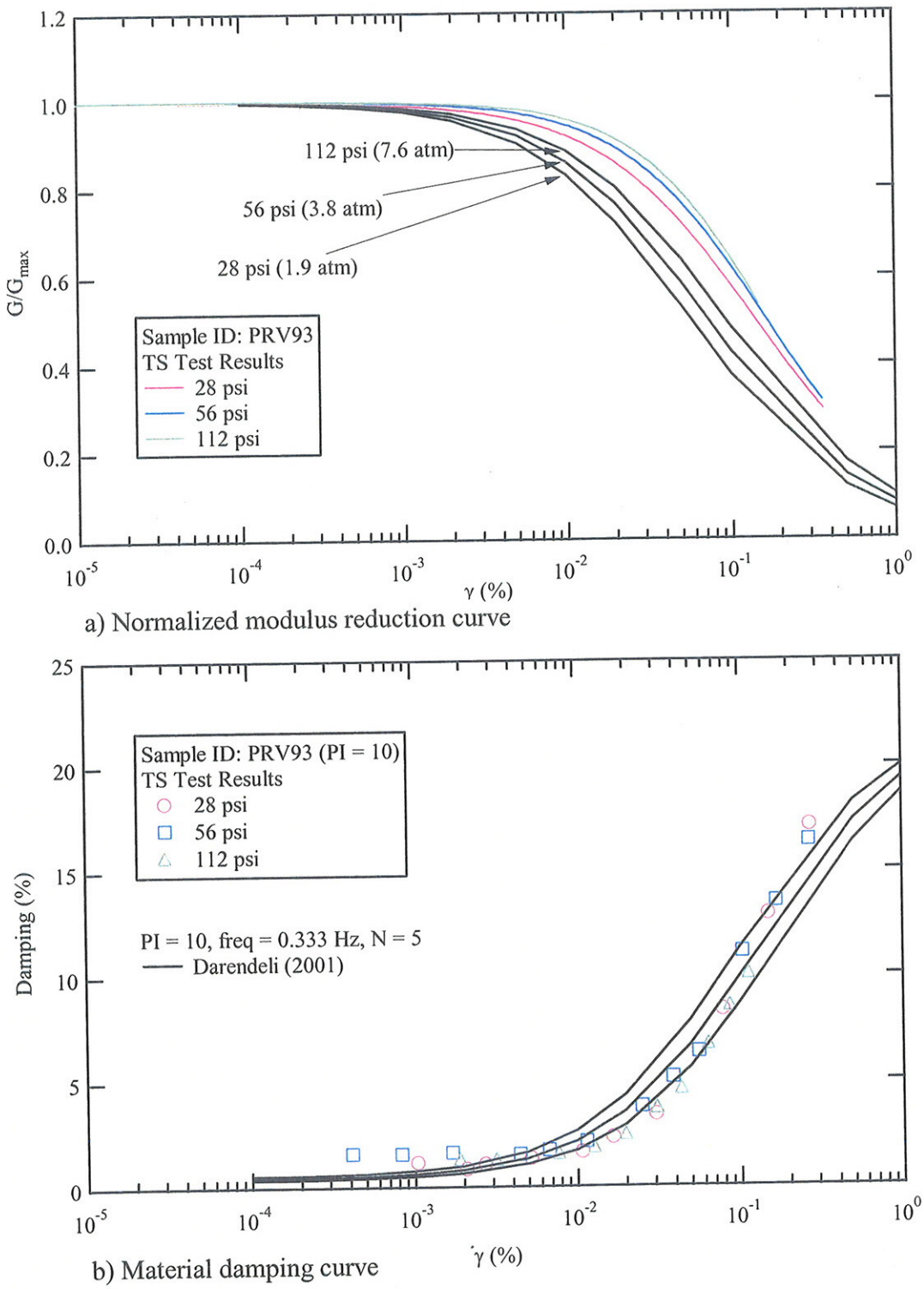

Figure 31 Comparison of confining pressure effects from TS tests on specimen PRV93 and curves proposed by Darendeli (2001)

5.3 Recommended Empirical Relationships for Bonneville Clay

The overall behavior of Bonneville clay was found to behave more linearly than was predicted by the empirical curves for behavior of typical clay at the same values of PI. If the empirical curves proposed by Vucetic and Dobry (1991) and Darendeli (2001) are used to predict the modulus reduction and damping curves, the values of PI should be corrected to provide the better match between the empirical curves and the actual behavior of Bonneville clay. The recommendations for correcting PI for both empirical relationships are presented below.

The modulus reduction curves predicted by Vucetic and Dobry (1991) show better agreement with the behavior of Bonneville clay when the values of PI increase by 10. Comparison of modulus reduction and damping curves for before and after correcting PI values are shown in Figures 32-35. The modulus reduction and damping curves of Bonneville clay presented in Figures 32-35 were generated for PI of 2, 10-11, 17, and 34. The Vucetic and Dobry (1991) curves were generated for the same values of PI and for the PI values of 12, 21, 27, and 44. Correcting for PI values show improvement in predicting modulus reduction curves for all specimens and the best results were observed for specimens with PI values of 17 and 34. For damping curves, correction of PI values to generate the Vucetic and Dobry (1991) damping curves shows less effective than the modulus reduction curves. This is due to the undefined damping curves from Vucetic and Dobry (1991) at low to medium strains.

Effect of PI on the modulus reduction curves predicted by Darendeli (2001) is similar to the behavior of Bonneville clay. However, the Darendeli (2001) curves pronounce more nonlinearly than the actual behavior of Bonneville clay. Correction of PI when using the Darendeli (2001) curves is recommended in this study. The relationship of actual PI value and recommended PI value used to generate the Darendeli (2001) curve that provide the best match to the behavior of Bonneville clay is shown in Figure 36. The PI values used for the Darendeli (2001) model should be increased linearly with the actual PI values of Bonneville clay. Linear relationship determined based on the results of this study is presented in Figure 36. The corrected PI values can be calculated and used to generate the modulus reduction and damping curves proposed by Darendeli (2001). Comparison of modulus reduction and damping curves for before and after correcting PI values are shown in Figures 37-40. Significant improvement in predicting modulus reduction curves and slight improvement in predicting damping curves was observed for all soil specimens. Modulus reduction and damping curves predicted by Darendeli (2001) using the PI correction provides better match to the measured curves than the curves predicted by Vucetic and Dobry (1991).

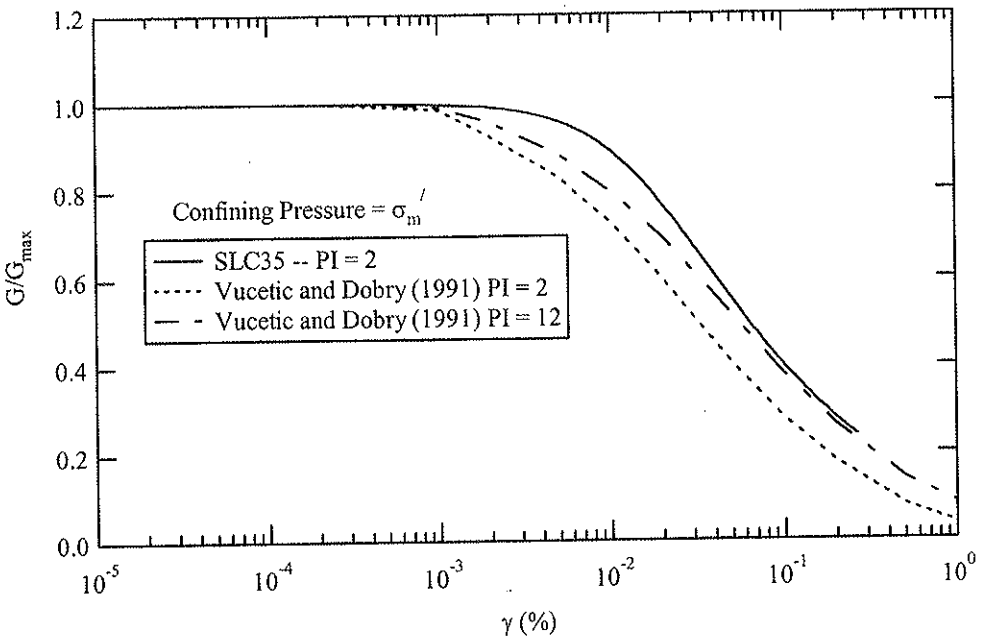

a) Modulus Reduction Curves

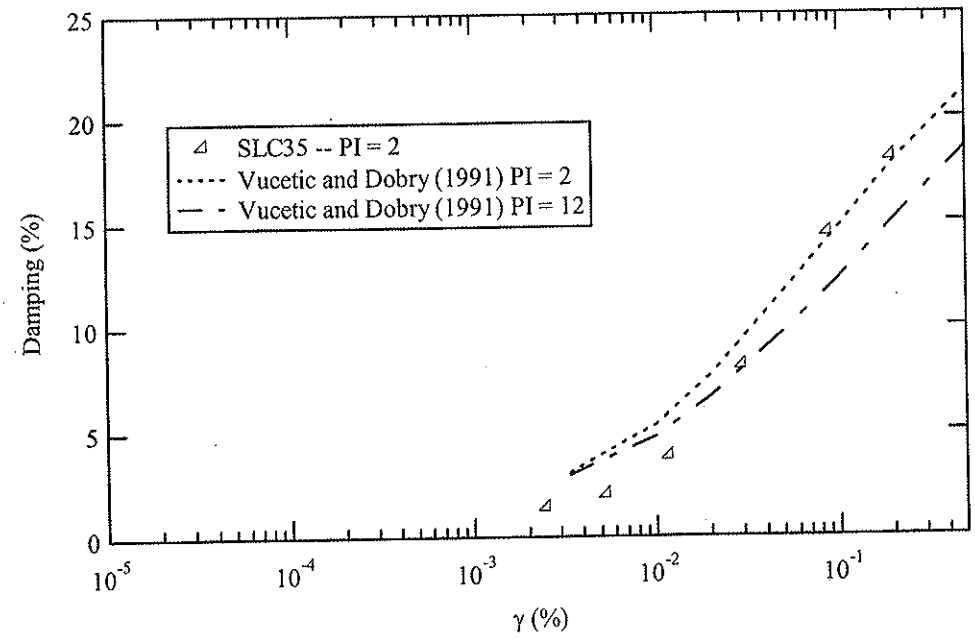

b) Damping Curves

Figure 32 Comparison of modulus reduction and damping curves on specimen SLC35 and curves proposed by Vucetic and Dobry (1991) before and after correcting PI values

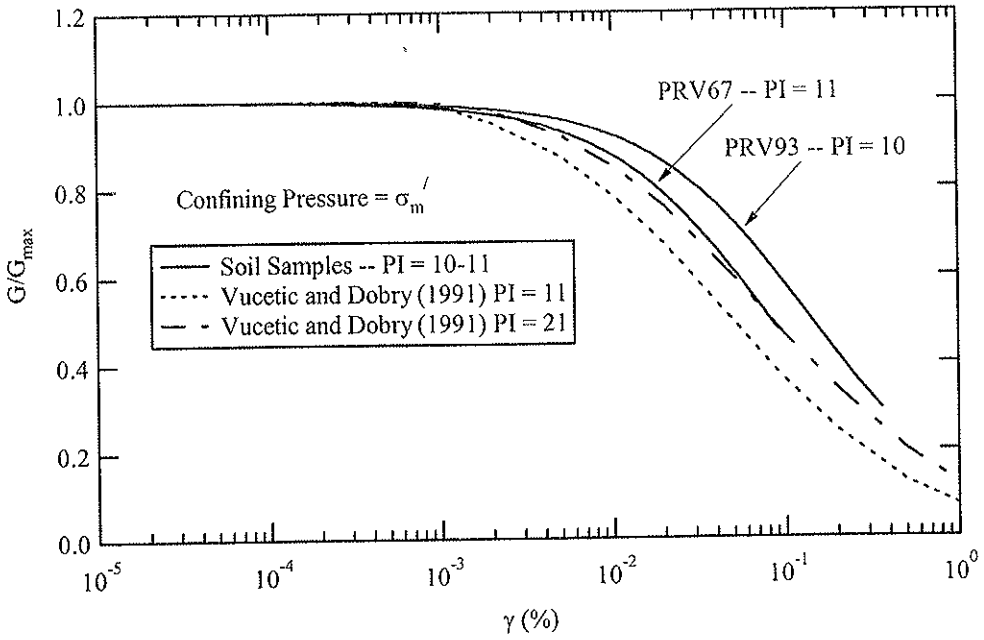

a) Modulus Reduction Curves

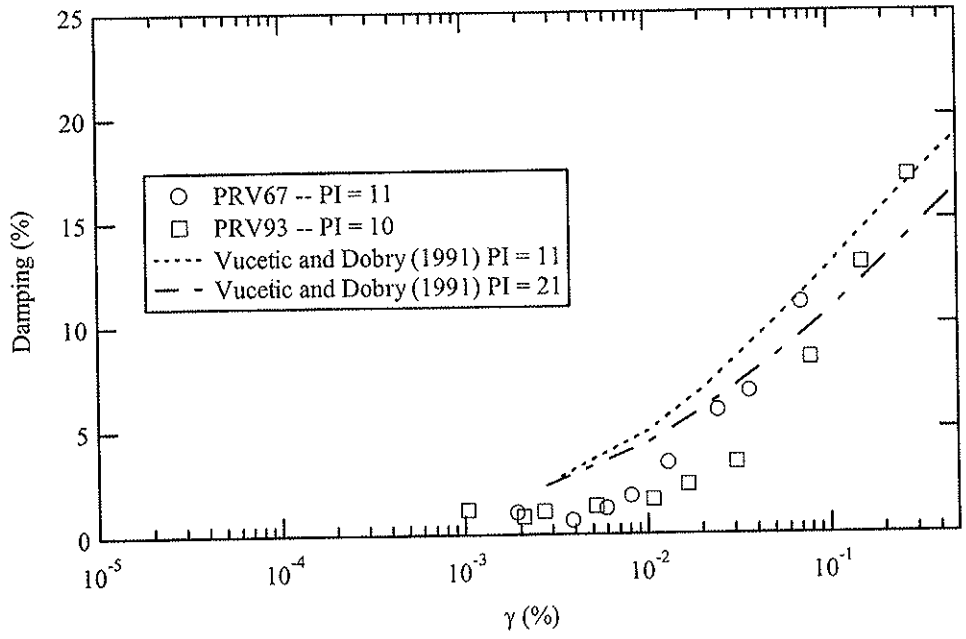

b) Damping Curves

Figure 33 Comparison of modulus reduction and damping curves on specimen PRV67 and PRV93 and curves proposed by Vucetic and Dobry (1991) before and after correcting PI values

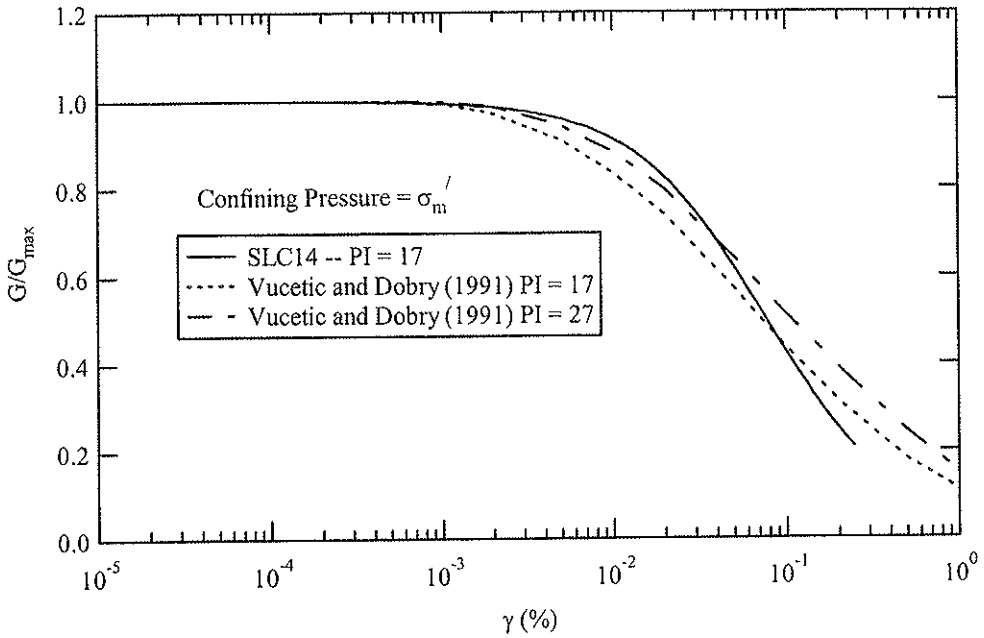

a) Modulus Reduction Curves

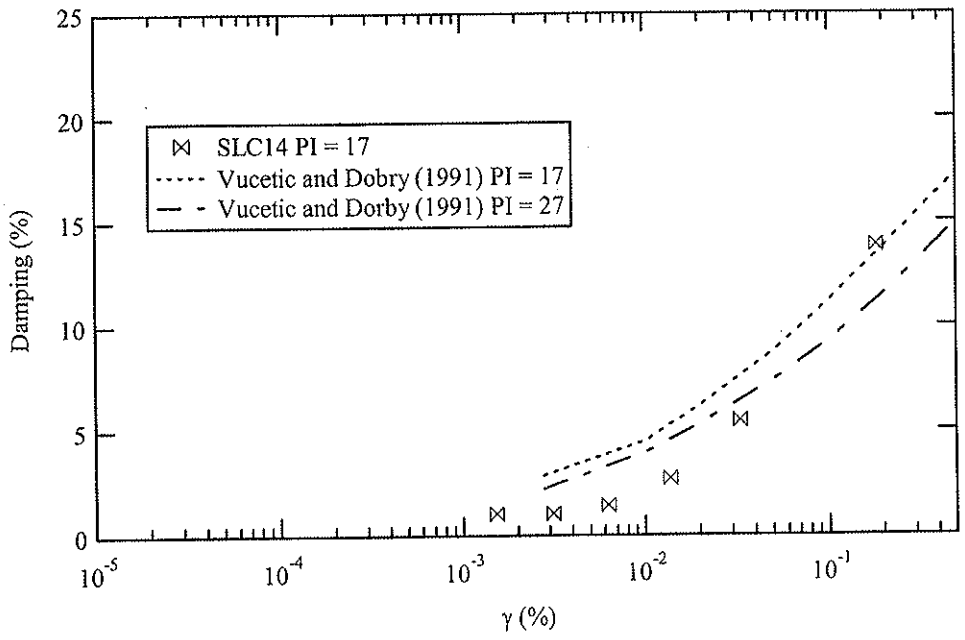

b) Damping Curves

Figure 34 Comparison of modulus reduction and damping curves on specimen SLC14 and curves proposed by Vucetic and Dobry (1991) before and after correcting PI values

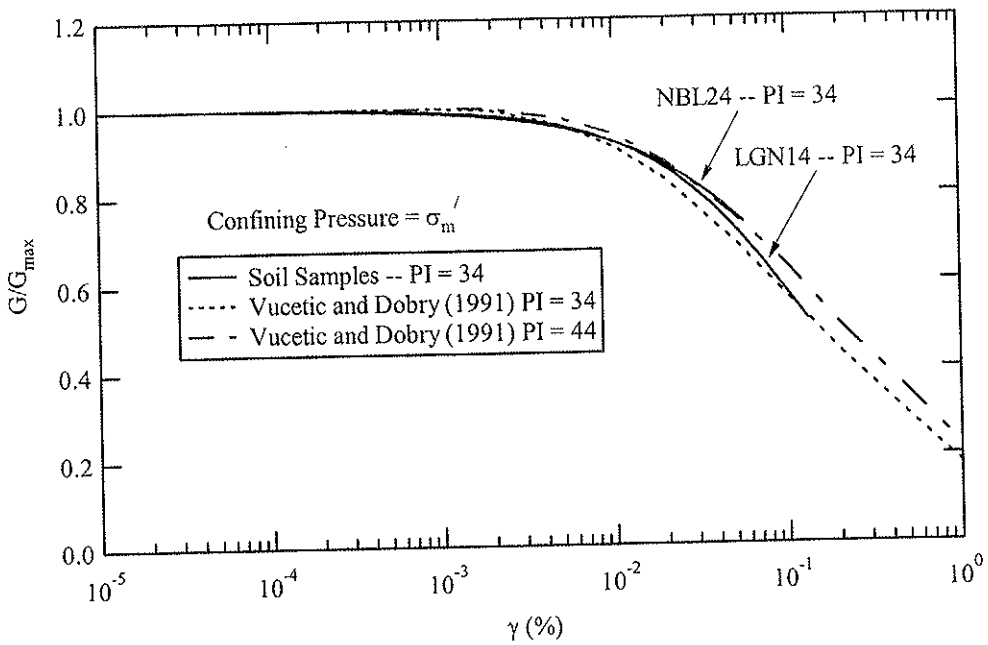

a) Modulus Reduction Curves

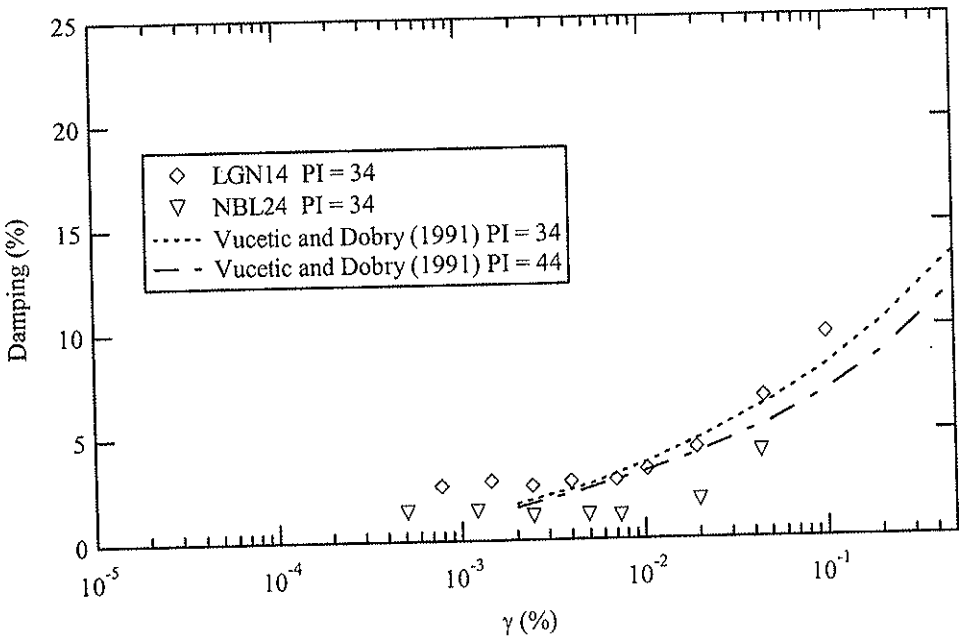

b) Damping Curves

Figure 35 Comparison of modulus reduction and damping curves on specimen LGN14 and NBL24 and curves proposed by Vucetic and Dobry (1991) before and after correcting PI values

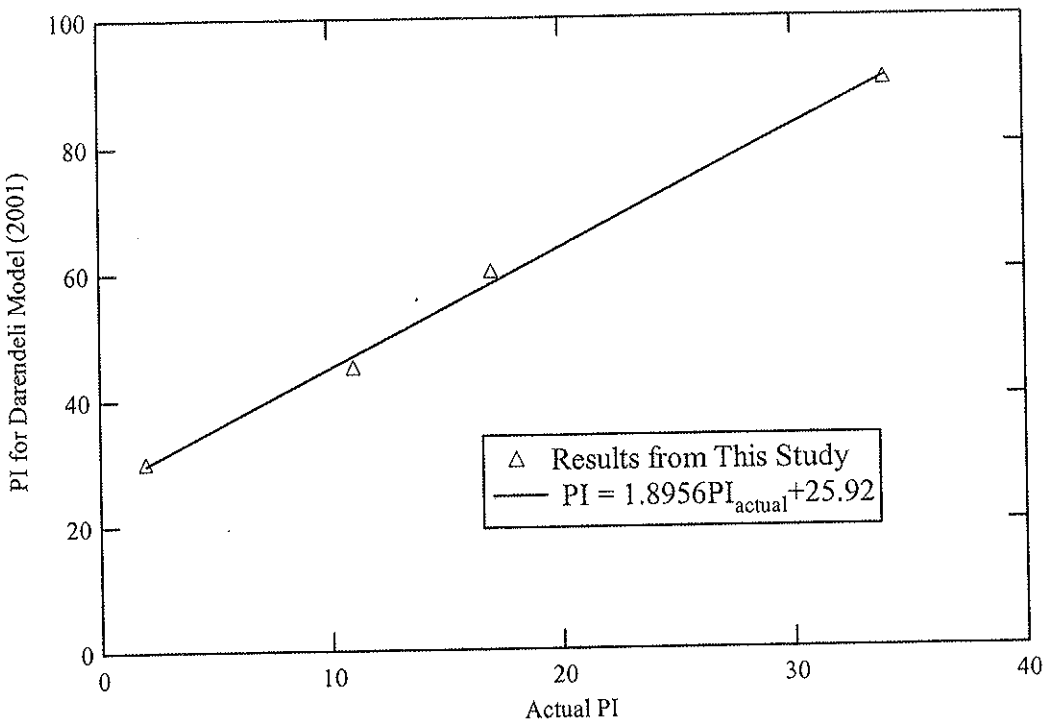

Figure 36 Correction of PI for predicting modulus reduction and damping curves using Darendeli (2001)

5.4 Conclusions

The overall behavior of Bonneville clay was found to behave more linearly than was predicted by the empirical curves for behavior of typical clay at the same values of PI. Less confining pressure effect was also observed for Bonneville clay. The empirical curves proposed by Darendeli (2001) provide the best match with the behavior of Bonneville clay. The more linear behavior of the Bonneville clay may be explained by geologic age effect. Bonneville clay is a relatively young soil, deposited 12,000-20,000 years ago during the Quaternary period. Zhang et al. (2004) compared modulus reduction curves from three groups of soils: Quaternary, Tertiary and older, and residua/saprolite. They found that Quaternary soils exhibit more linearity than soils of the other two groups. They also observed that most of the soils used to develop the Darendeli (2001) model are Tertiary soils. Accordingly, Zhang et al. (2004) showed a better agreement between the Darendeli (2001) model and Tertiary age soils than the Darendeli (2001) model and Quaternary soils. Correcting empirical relationships by increasing PI may provide more accurate modulus reduction and damping curves of Bonneville clay.

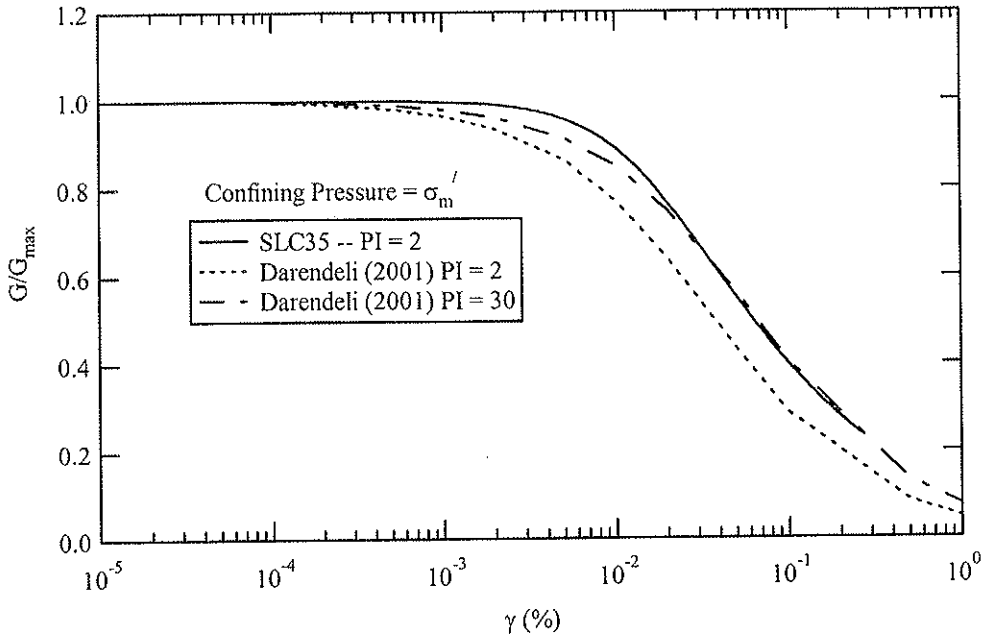

a) Modulus Reduction Curves

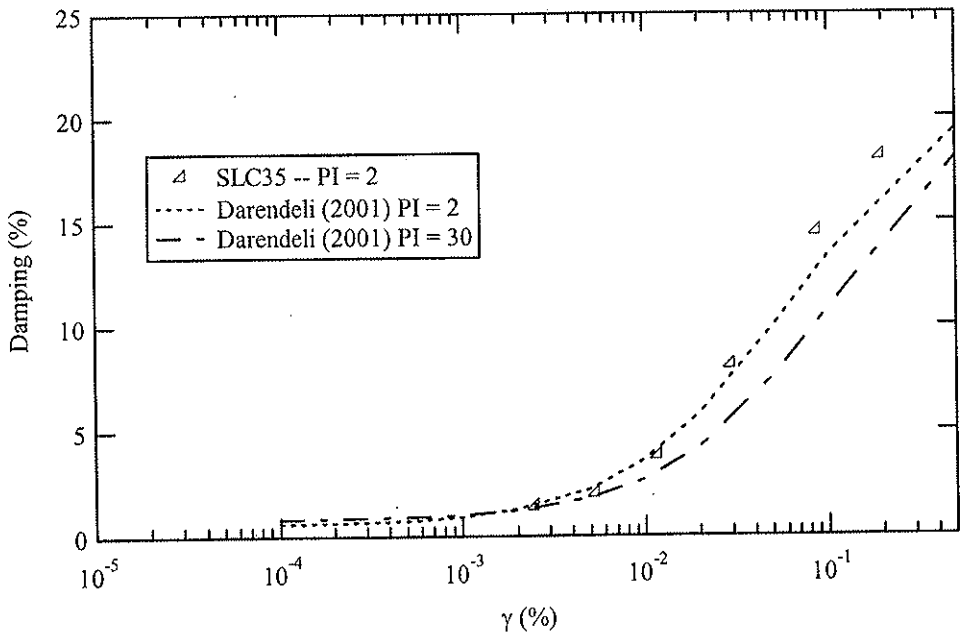

b) Damping Curves

Figure 37 Comparison of modulus reduction and damping curves on specimen SLC35 and curves proposed by Darendeli (2001) before and after correcting PI values

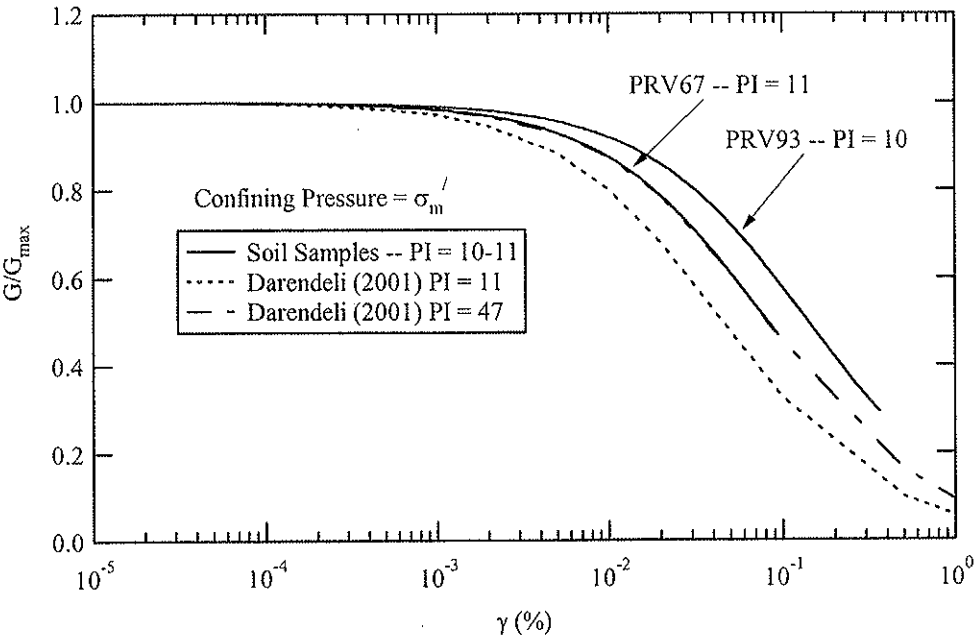

a) Modulus Reduction Curves

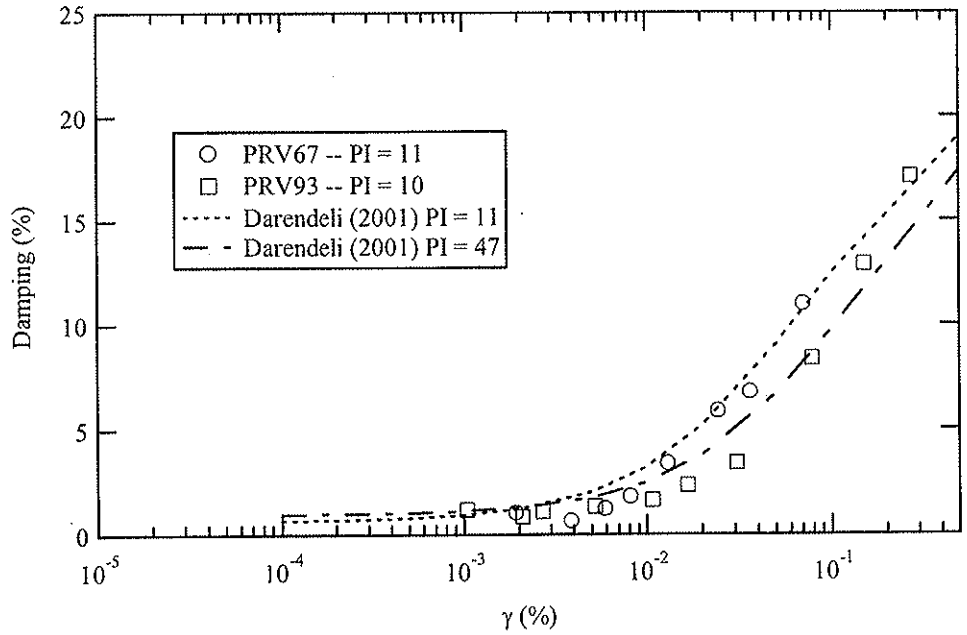

b) Damping Curves

Figure 38 Comparison of modulus reduction and damping curves on specimen PRV67 and PRV93 and curves proposed by Darendeli (2001) before and after correcting PI values

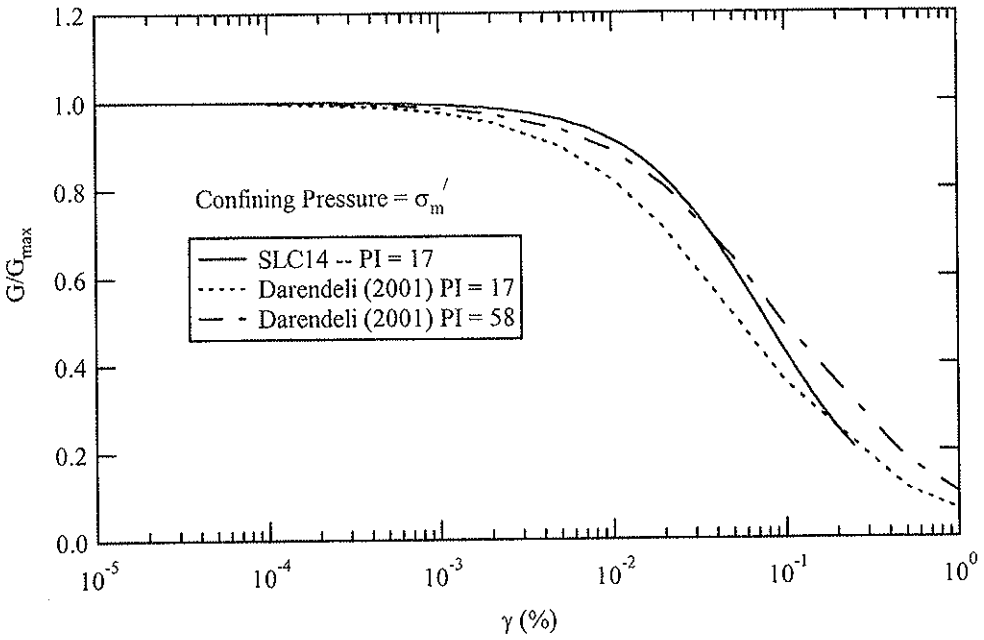

a) Modulus Reduction Curves

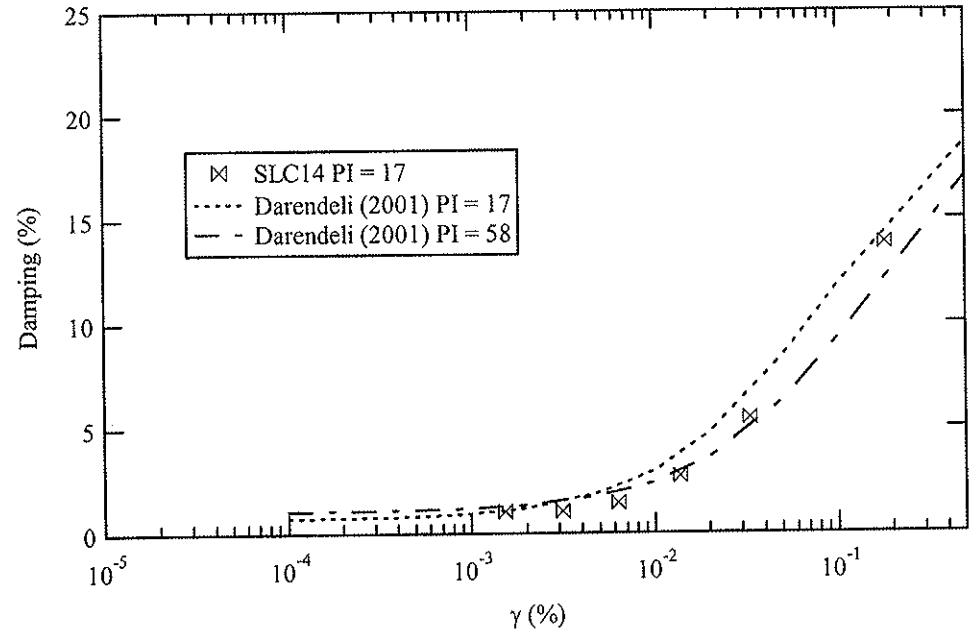

b) Damping Curves

Figure 39 Comparison of modulus reduction and damping curves on specimen SLC14 and curves proposed by Darendeli (2001) before and after correcting PI values

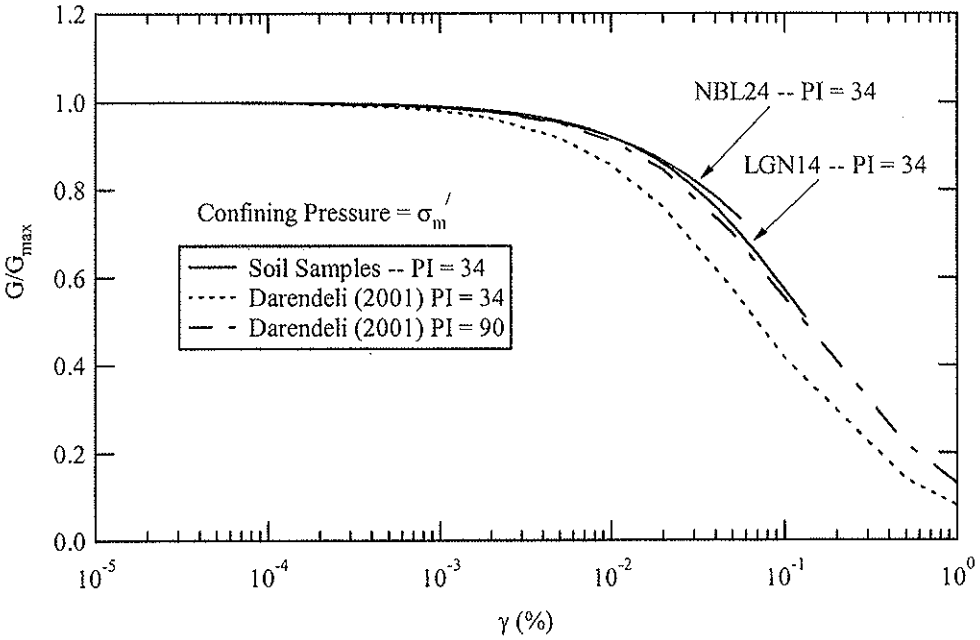

a) Modulus Reduction Curves

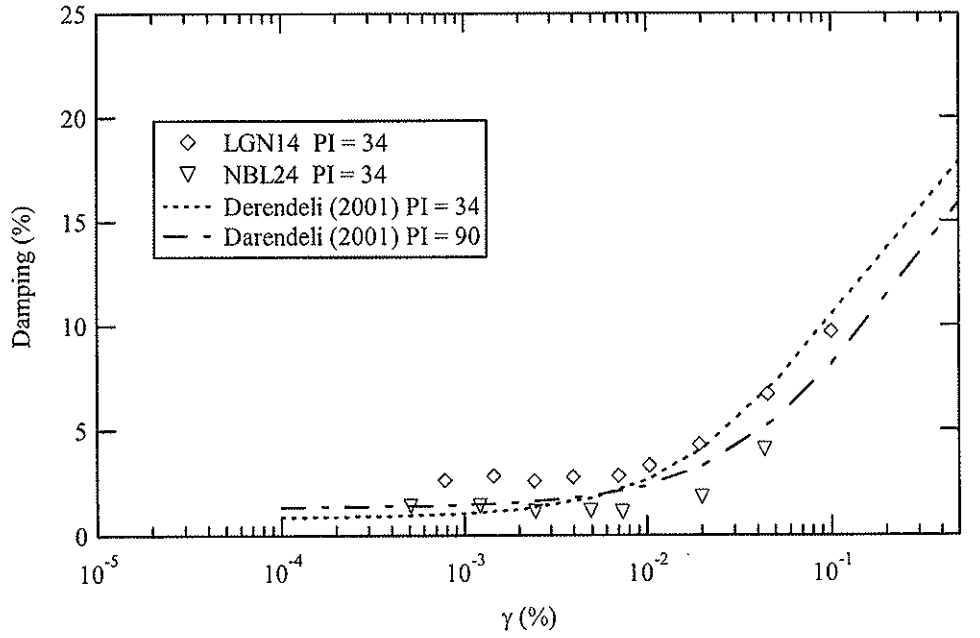

b) Damping Curves

Figure 40 Comparison of modulus reduction and damping curves on specimen LGN14 and NBL24 and curves proposed by Darendeli (2001) before and after correcting PI values

REFERENCES

Darendeli, M. B. (2001). "Development of a new family of normalized modulus reduction and material damping curves," PhD dissertation, Univ. of Texas, Austin, Tex.

Kim, D. S. (1991). "Deformational characteristics of soils at small strains from cyclic tests," PhD dissertation, Univ. of Texas, Austin, Tex.

Sasanakul, I., (2005). "Development of electromagnetic and mechanical model for a resonant column and torsional shear testing device for soils," PhD dissertation, Utah State Univ., Logan, UT.

Sun, J. I., Golesorkhi, R., and Seed, H. B. (1988). "Dynamic moduli and damping ratios for cohesive soils." *Rep. UCB/EERC-88/15*, Univ. of California, Berkeley, Calif., 48.

Vucetic M., and Dobry, R. (1991). "Effect of soil plasticity on cyclic response." *J. Geotech. Engrg.*, ASCE, 117 (1), 89-107.

Zhang, J., Andrus, R. D., and Juang, C. H., (2005). "Normalized shear modulus and material damping relationships." *J. Geotech. and Geoenviron. Eng.*, ASCE. (In press).